Quaternary Science Reviews 177 (2017) 173–188

Contents lists available at ScienceDirect

Quaternary Science Reviews

journal homepage: www.elsevier.com/locate/quascirev

Lake-level stratigraphy and geochronology revisited at Lago (Lake) Cardiel, Argentina, and changes in the Southern Hemispheric Westerlies over the last 25 ka

J. Quade [a, *], M.R. Kaplan [b]

[a] Department of Geosciences, University of Arizona, Tucson, AZ 85721, USA
[b] Geochemistry, Lamont-Doherty Earth Observatory of Columbia University, New York 10964-8000, USA

ARTICLE INFO

Article history:
Received 10 January 2017
Received in revised form
29 September 2017
Accepted 3 October 2017

Keywords:
Quaternary
Paleoclimatology
South America
Lakes
Carbon-14 dating
Tufa

ABSTRACT

Paleoshorelines around Lago (Lake) Cardiel in southern Argentina (S48.9°, W71.3°; ~275 m) record substantial changes in lake area over the past 25 ka. Our results combined with previous research show that during the last glacial maximum (or LGM, 23–21 ka), the lake stood at near modern levels, but had nearly dried up by ~13 ka. Between 11.3 and 10.1 ka the lake reached its highest point (+54–58 m) and greatest extent in at least the last 40 ka. Lake levels dropped thereafter and experienced two lower-lake periods: 8.5–7.5 ka and 5–3.3 ka; and two higher-lake periods: 7.4–6 and ~5.2 ka. In the last 3.5 ka, the lake has remained generally near or slightly above its present level.

The depth and surface area of Lago Cardiel are controlled mainly by precipitation onto the lake and surrounding catchment, air and water temperature, and wind-speed related to local strength of the Southern Hemispheric Westerlies (SHW). Our lake-level reconstruction combined with evidence from other studies suggest that on average the core of the SHW was located well to the north (<45°S) of the Cardiel basin during the deep lake phase associated with the LGM, and was well to the south (>55°S?) during the hydrologic maximum of Cardiel in the early Holocene. The lower phases of the lake at 20.0–11.5, 8.5–7.5, and 5.0–3.3 ka generally correspond to cold conditions in other records, when we infer that the SHW were strongly focused around the latitudes of Cardiel at 49°S.

1. Introduction

Lake records have made a fundamental contribution to our understanding of the Earth's changing moisture state during the Quaternary. Past fluctuations of a hydrographically closed lake constitute a clear record of changes in moisture balance within that lake's drainage basin. These changes, in turn, can be used in concert with other paleoclimatic records to infer past shifts in atmospheric circulation. For example, closed-lake systems and other records show that the temperate mid-latitudes in both hemispheres experienced episodes markedly wetter conditions than today during last full to late-glacial period 23–12 ka (Oviatt et al., 1992; Moreno et al., 1999; Benson et al., 2013; Torfstein et al., 2013). But there are also some intriguing exceptions to this global pattern, such as the subject of this study, Lago Cardiel in southern (48.9°S) South America (Fig. 1), where Stine and Stine (1990) showed that this lake rose to its highest levels 11–10 ka, markedly later than nearly all other lakes in the mid to high latitudes.

Similar to the study of Stine and Stine (1990), we focused on the evidence from paleoshorelines and other naturally exposed lake deposits to reconstruct changes in lake size. The study of shorelines has the advantage over core-based studies in that lake levels are not inferred through various proxies but by direct observation, visually where the shorelines are exposed, or seismically where paleoshorelines are submerged. The seismic evidence is especially vital at Lago Cardiel, because the lake today is closer to its hydrologic maximum than minimum, and therefore submerges most of the pre-modern shorelines (Gilli et al., 2005a). Lake area is easily determined in shoreline studies, a key term in hydrologic mass balance equations that allows reconstruction of precipitation required to grow or shrink lakes (e.g. Kutzbach, 1980; Placzek et al., 2013). The main disadvantage of shorelines is the incomplete nature of the record, caused by erosion of older deposits during lake transgressions and regressions. Hence, multiple sites must be

* Corresponding author.
E-mail address: quadej@email.arizona.edu (J. Quade).

https://doi.org/10.1016/j.quascirev.2017.10.006
0277-3791/

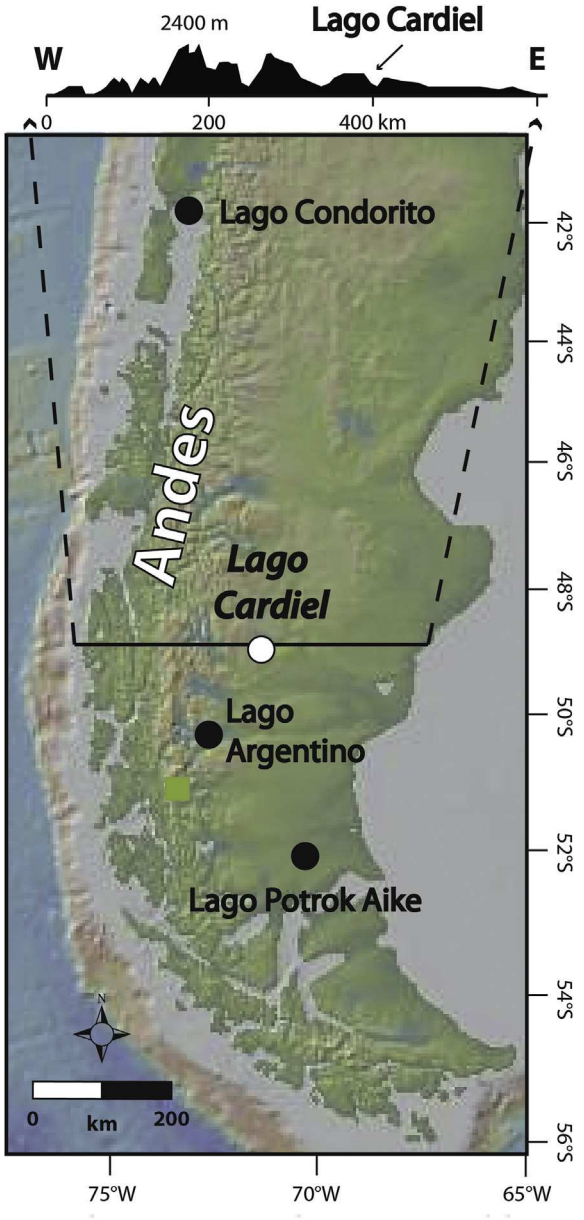

Fig. 1. Regional map and topographic profile showing the location of Lago Cardiel east of the Andes in southern South America. Also shown are Lagos Condorito, Argentino, and Potrok Aike discussed in the text.

studied in order to fill in the stratigraphic gaps. The shorelines at Lago Cardiel are well preserved and amply exposed, providing many opportunities for dating and stratigraphic replication.

The lake record at Lago Cardiel has already been studied from a variety of perspectives. Galloway et al. (1988) but especially Stine and Stine (1990), were the first to study the lacustrine deposits around Lago Cardiel. Stine and Stine (1990) focused on a fairly small area, mainly mapping and dating of deltaic deposits naturally exposed in the walls of stream cuts along the Rio Cardiel, Rio Bayo, and Arroyo Cerro Goro (Fig. 2). Terrestrial organic matter is abundant in these deltaic deposits, providing a firm basis for dating the lake-level fluctuations. Wenzens (2005) documented possible shorelines much higher than those identified by previous work, which he speculated were produced by discharge into the basin by a diversion of Rio Chico along the Tres Lagunas Valley (Fig. 2). In addition to shoreline deposits, another advantage of Lago Cardiel is that it has a rich subsurface record that can be synthesized with former lake-level findings, from two coring efforts (Gilli et al., 2001; Markgraf et al., 2003), and by seismic imaging (Gilli et al., 2005a; Beres et al., 2008).

Despite prior work, the exposed lake deposits around Lago Cardiel still constitute a prime opportunity for further study and replication, since there are many unstudied localities at multiple paleolake levels which record the details of the repeated rise and fall on lake. Our intent in this paper is to revisit Lago Cardiel, test and build on the lake level reconstruction of Stine and Stine (1990) and Wenzens (2005) with significantly more sampling and dating, merge the shoreline observations with that of the core records, and interpret the lake record in terms of an up-to-date understanding of the changing position or strength of the Southern Hemispheric Westerlies (or SHW) and changing temperature over the past 25 ka.

2. Lake Basin characteristics and modern climate

Lago Cardiel lies at 48.9°S and 71.2°W in Santa Cruz province of southern Patagonia (Figs. 1 and 2). The current lake level is at ~275 masl, and the lake is ~75 m deep, covers 370 km^2 in area, and occupies ~8% of the catchment basin encompassing ~4500 km^2 in area. High-standing plateaux or "mesetas" underlain by mostly late Neogene basalts (Ramos, 1982) hydrographically isolate the Cardiel basin from the Andes to the west. Reaching 1940m in elevation, the mesetas supply most of the recharge to the basin. Rio Cardiel, the main inflow into Cardiel today, heads in the mesetas, as does the smaller Rio Bayo. The Cardiel area has not been glaciated on the timescale of this study, perhaps since the Miocene (Wenzens, 2006).

The Lago Cardiel basin is cold due to its high latitude and interior position, with a mean annual temperature of 7.5 °C. It lies in the rain shadow of the Andes and so is quite dry, with a mean annual precipitation 210 mm/yr, even though Cardiel lies near the center of the modern SHW, due to orographic blockage of SHW precipitation by the Andes as well as perhaps the Southern Patagonian Ice Field to the west. Vegetation in the basin around the lake is treeless shrub steppe (or Patagonian steppe of Mancini et al., 2008).

Lago Cardiel, at 48.9°S, lies within the main belt of the SHW between 43 and 53°S. The core position shifts by ~ 5–6° seasonally. In summer, the SHW are more narrowly focused between ~50 and 55°S, and austral summer winds in Patagonia around the latitude of Cardiel are stronger. In winter precipitation belt expands northwards to ~35–40°S (Fig. 3; Lawford, 1996; Lamy et al., 2010), and with this broadening, winter winds slacken. Precipitation from moist marine air carried by the SHW makes the western flank and high passes of the Andes in southern Chile one of the wettest (mean annual precipitation = 4000–11,000 mm/yr) and cloudiest regions in the world (Schneider et al., 2003). The SHW lose most of their moisture before reaching the eastern side of the Andes where they descend and warm, reducing precipitation to ~210–250 mm/yr at Lago Cardiel (Heinsheimer, 1958). The dry but strong SHW dominate the "foehn" or "zonda" winds in this region, falling in the 4–8 m/s range (Heinsheimer, 1958; Schneider et al., 2003).

Garreaud (2007) has pointed out that strong SHW winds, at both low and high tropospheric levels, tend to promote precipitation on the windward side of the southern Andes but suppress it on the leeward side. Barros and Mattio (1978) and Stine and Stine (1990) appear to be the first to stress the importance of the Atlantic over the Pacific Ocean as the main source of moisture east of the Andes in eastern Patagonia. Further evidence presented in Schneider et al. (2003), Mayr et al. (2007), Moy et al. (2008), and most comprehensively in Agosto et al. (2015) demonstrate that in fact rain and snow falling east of the Andes at this latitude come dominantly from the Atlantic and are borne by easterly, not

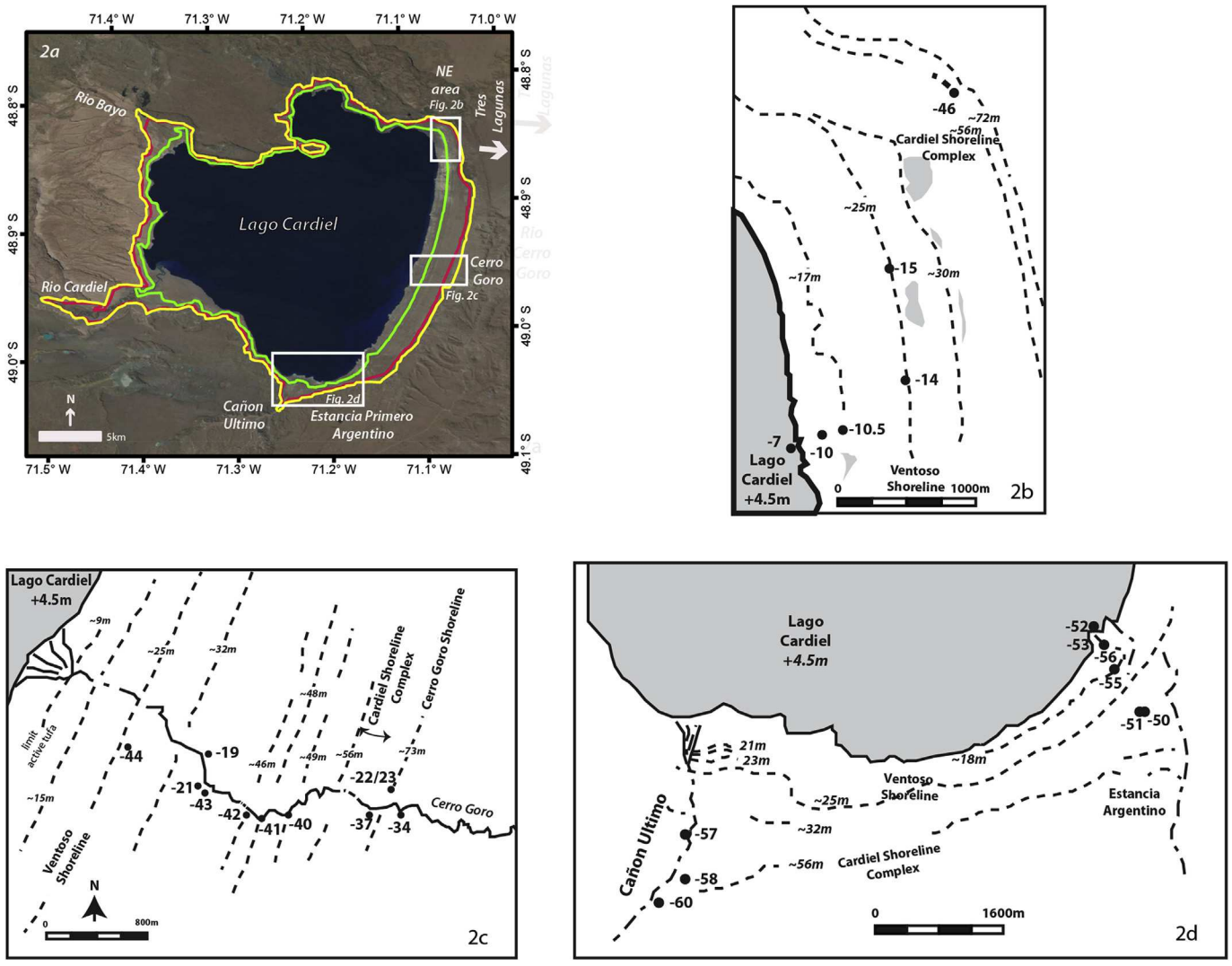

Fig. 2. a. General map of the Lago Cardiel area showing the approximate trace of the +21–22 m (green–Ventoso Shoreline), +54–58 m (red–Cardiel Shoreline Complex), and +73–75 m l (yellow–Cerro Goro Shoreline) paleoshorelines. The direction of the spillway in the Tres Lagunas area of Wenzens (2005) is also indicated. Boxed areas encompass the major sampling transects shown in Fig. 2: 2b. (NE area), 2c. (Arroyo Cerro Goro area), 2d. (Estancia Primero Argentino and Cañon Ultimo area). In these boxed areas, we indicate the sample locations (Table 1), main paleoshorelines with estimated elevations relative to the 1988 lake level (dashed lines), and main areas of standing water (gray shaded).

westerly winds. This creates a dipolar precipitation pattern across the Andes at this latitude of South America: the strong SHW lead to very wet conditions on the west side of the Andes, but dry conditions to the east. When the SHW slacken, more easterly moisture can reach the area of Lago Cardiel, making it wetter and generally less windy. The relationship of precipitation to the strength of the SHW is also evident in seasonal precipitation patterns; although there is not a very pronounced dry season, most precipitation comes out of the Atlantic Ocean in the austral spring and fall months when the SHW are weaker and the core is shifted north of 50°S (Lamy et al., 2010).

3. Lake deposits

3.1. Shorelines

Our investigations focused on natural exposures of deposits associated with the paleoshorelines fringing the basin. There are many shorelines but three are especially widespread and topographically conspicuous. Stine and Stine (1990) designated them as the +75 m, +55 m, and +21.5 m shorelines, with +0 m being the lake level in January and February 1988. To standardize future nomenclature we have named these three paleoshorelines (Fig. 2a), following the practice of paleolake studies in many other basins (e.g. Morrison, 1965; Oviatt et al., 1992; Placzek et al., 2006). These include the highest and oldest shoreline at +72 to +75 m which we name the Cerro Goro shoreline, after the location where it is best exposed. The Cardiel shoreline complex is composed of three closely related shorelines in the +54 to +58 m range, lower than the Cerro Goro shoreline, and conspicuously better preserved. Last, we designate the tall shoreline berm at +21 to +22 m as the Ventoso shoreline, the best preserved and the youngest of the prominent shorelines around Lago Cardiel. Natural exposures of beach deposits in these shorelines are common in the basin, but we chose to focus our work on three areas on the east side of the lake where exposure is most continuous and ^{14}C-datable shell and tufa are common: along Cerro Goro and Cañon Ultimo, near Estancia Argentino, and in the NE corner of the lake among a series of isolated exposures (Fig. 2). Select exposures along Cerro Goro were also studied by Stine and Stine (1990) but not in the other areas; as

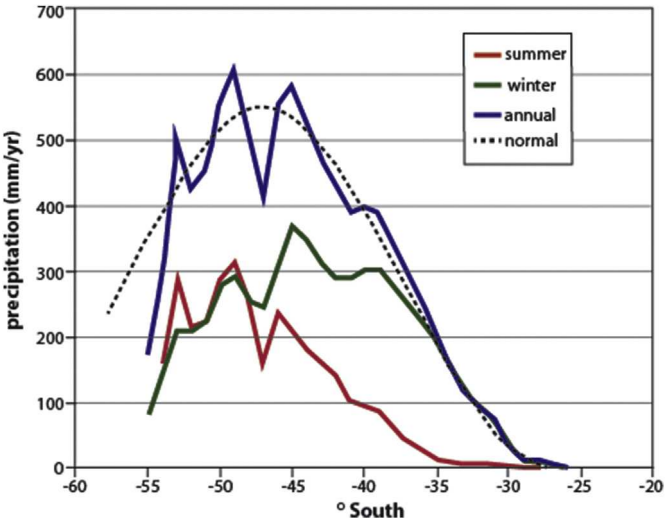

Fig. 3. Distribution of precipitation in western Chile (mm/yr) by latitude (°S) during summer, winter, and annually. Also shown as a dashed line is the normal best fit to the annual amounts. Modified from Lawford (1996).

mentioned in the introduction, we focused mainly on new exposures and sites, which complements previous work.

3.2. Sedimentology and dating

Exposed lake deposits fall into three general sedimentologic categories: (1) well-rounded and often shingled gravels (Fig. 4b), and cross-bedded sands formed in high energy conditions in the nearshore, often associated with aquatic shell (Fig. 4b, f), (2) a variety of forms of tufa and cemented beach rock also formed in shallow water and nearshore environments (Fig. 4a, c-d), and (3) laminated silt (Fig. 4e and f) deposited in low-energy lagoonal or off-shore settings. Aquatic shell from the beach sands (Fig. 4b, f) forms the main basis for our extensive ^{14}C dating campaign (Table 1).

Tufas at Lago Cardiel are composed of porous to densely cemented carbonate (Fig. 4a). Total thicknesses range widely, from up to 20–30 cm to more typically a few centimeters. Tufa form also varies widely (Fig. 4). Most is cemented onto local beach boulders, and is rough on the surface, rather like the appearance of cauliflower. Nearest the present lake, cementation can be continuous between rocks, forming well-cemented beach rock (Fig. 4 c–d). Higher in elevation, fossil tufa heads are isolated around individual boulders, and are rare above +12 m. However, tufas are not usually associated with a discernable shoreline. Partly this has to do with the fact that the lake appears to have fluctuated through the zone 0 to +12 m repeatedly, and each lake cycle has remodeled shorelines and buried older deposits, obscuring associations. Shells are sometimes cemented into the tufa. Layering (Fig. 4a) is apparent in most tufa, distinguished by color and texture along readily breakable surfaces that appear to represent hiatuses in deposition. Tufa is forming today in the lake shallows and we detected bomb-carbon in several thin tufa coatings near the modern lake level (Fig. 4c).

Lacustrine tufa tends to form in the photic zone usually in association with photosynthetic algae. In some clear lakes the photic zone is deep and thus tufa can form down to 20 m depth (e.g. Brady et al., 2010). In turbid waters mixed constantly by wind, such as at Lago Cardiel, the photo zone in shallow and in our experience from turbid lakes in Tibet (e.g. Hudson et al., 2015) and the western US, the tufa forms within a few meters of the lake surface. This makes most tufa an excellent means for constraining minimum lake surface elevations to within a few meters of the true elevation. Layering and stratigraphic breaks in the tufa denote the rise and fall of the lake through the photic zone. Although primarily based on ^{14}C dating of aquatic shell, which dates the shoreline directly, in this study we also ^{14}C date tufas, mainly to reconstruct the times when the paleolake stood at or just above the modern lake.

4. Methods

4.1. Elevation estimates

Shoreline elevations were measured by two hand-held Garmin GPSs equipped with a barometric altimeters. We reset them to the lake level each morning before the winds began to rise, and found our elevation measurements to be reproducible at ±1 m. The barometric-based elevation estimates of most sample locations were checked using a hand-held abbey level, relative to the then modern (2010) lake level.

The Ventoso shoreline is conspicuous and well preserved feature that we used to relate our elevations to those of Stine and Stine (1990). Stine and Stine (1990) placed the Ventoso shoreline at +21.5 m above the lake level in the late 1980s. We used Abney level to estimate the height of this shoreline at over five locations and consistently obtained +16.5–17 m above the 2010 lake, suggesting that the lake has risen by 4–5 m since the late 1980's. Despite this difference, we report all our elevations in this paper relative to the elevation of lake when Stine and Stine (1990) conducted their study. And thus, the lake at the time of our study in 2010 appears to have been at +4.5 m relative the lake in the late 1980's.

4.2. Dating

All sample preparation prior to AMS measurement was performed at our in-house ^{14}C laboratory at University of Arizona. All tufa subsamples and shells were rinsed ultrasonically to remove detritus and reacted in 3% H_2O_2 to remove organic material. Clean samples of shell free of secondary cements or detritus were selected for dating. Typically, only one valve was required. Tufa was slabbed on a rock saw and washed in distilled water. Areas of dense carbonate visibly free of secondary cement were selected for dating. Individual layers were clearly discernible in many tufa samples, and we focused our subsampling on the individual layers. Chips were detached using a second small rock saw.

Each sample was reacted with 100% H_3PO_4 under vacuum until fully dissolved. Organic samples were subjected to a standard acid-base-acid treatment, and completely combusted under vacuum in the presence of Ag and CuO at 900 °C. Sample gas was extracted under vacuum, cryogenically purified and passed through a 600 °C Cu/Ag furnace to remove contaminant gases. Purified CO_2 samples were graphitized using 100 mg of zinc powder and Fe powder in a 2:1 proportion to the mass of carbon in the sample. AMS and $\delta^{13}C$ measurements were performed by the Arizona Accelerator Facility. Radiocarbon dates from our study and that of some older studies, such as Stine and Stine (1990), were calibrated using the Calib 7.1 software based on the IntCal13 calibration curve (Reimer, 2013), and all are reported in calendar years before present.

5. Results

5.1. Dating considerations

Fossil shell and tufa were the main materials available for dating, yielding over fifty new ^{14}C dates for the Lago Cardiel deposits. Macroscopic plant remains dated by Stine and Stine (1990)

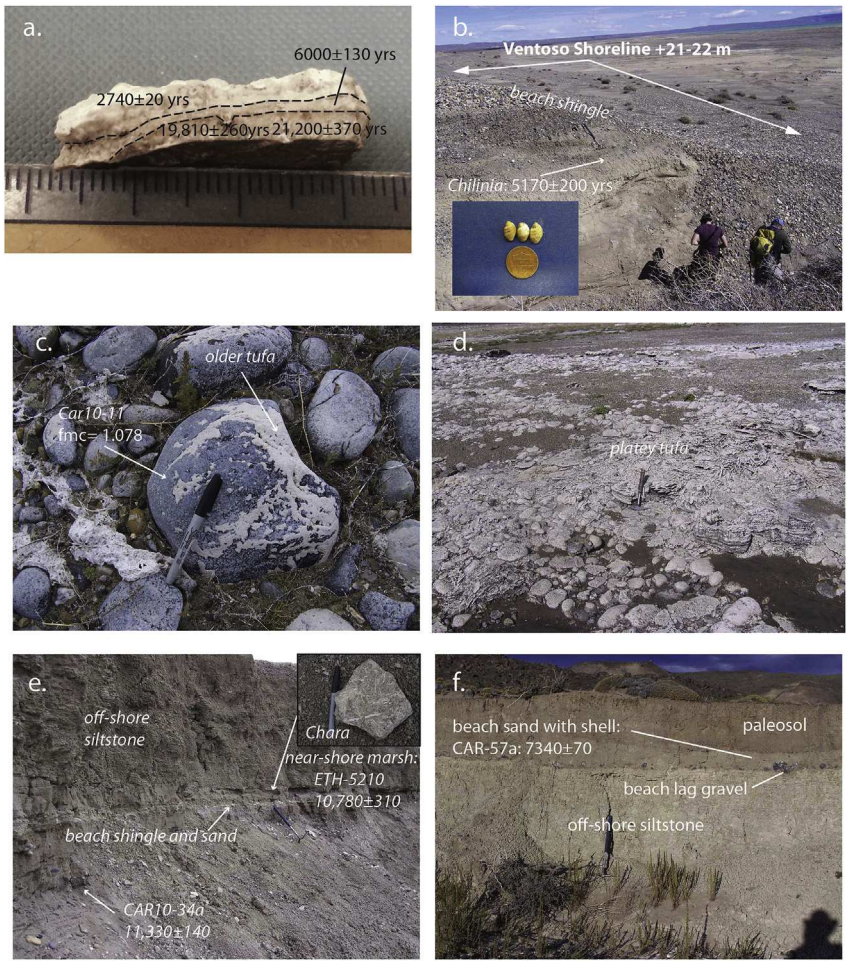

Fig. 4. Photographs from the Lago Cardiel area: a) cross-section of tufa sample CAR10-52c (+8 m) revealing three periods of tufa formation, scale increments 1 mm b) exposure of the prominent Ventoso shoreline (+21–22 m) at CAR10-14, with calibrated ^{14}C date on aquatic snail *Chilinia* shown in inset, as well as capping beach shingle, c) two generations of tufa from Car10-10 (+17.3 m; Table 1) with fraction modern carbon (fmc) indicated for the younger generation of carbonate frosting on basalt clasts; the older tufa at this site (Car10-11) yields a range of stratified early to late Holocene ages d) well-developed platey tufa at Car10-53 (+10; Table 1), 30 cm hammer for scale e) exposure at CAR10-34 (~+55 m at the elevation of the beach shingle) of a sequence marking the transgression to the Cardiel shoreline, consisting of a basal beach gravel and shingle, *Chara*-rich (shown in inset) silt originally dated to 10,780 ± 310 B.P. by Stine and Stine (1990), and an overlying undated deeper water silts, 1.1 m hammer for scale f) gravel lag deposited along surface during the regression from the Cardiel shoreline complex past +32 m at CAR10-57 in Cañon Último, with calibrated ^{14}C date shown (Table 1: CAR10-57a). Outcrop is 2 m high. All dates are expressed in cal yr B.P. or fraction modern carbon (fmc).

appear to be confined to deltaic deposits, and were not found in the shoreline deposits that we studied. Snails are living in the lake today. One sample near the mouth of the Rio Bayo contained a small bivalve (Sphaeridae), and several large (>2 cm) aquatic snails, including ornate *Chilina* sp. (Fig. 4b; Rumi et al., 2008), and several species of Lymnaeids. Fossil snails used for dating are almost entirely *Chilina* sp., which are common in Patagonian rivers, lakes, and springs. They are thick walled and generally one specimen was sufficient for ^{14}C dating. Fossil specimens are in excellent condition where they are not reworked. We selected samples free of secondary cements that often retained some of their original brown chevron coloring.

We obtained two samples of organic matter from the modern lake to evaluate the extent of equilibrium between carbon in the lake and atmosphere. From rotting algae collected along the lake margin we obtained fraction modern carbon (fmc) of 1.1325, and from assorted organic debris 1.025 (Table 1). These results bracket the assumed modern value for 2010 of about 1.06–1.08. A very thin coating of recent tufa associated with abraided bottle glass about ~3.5 m above the current (2010) lake returned a value of 1.078 (Table 1; Fig. 4c, Car10-11). These results indicate that ^{14}C dissolved in the lake is at or near isotopic equilibrium with the atmosphere. This conclusion is bolstered by measurements of ^{14}C of aquatic plants (*Ruppia*) and algae sampled ca. 1998 which returned a fraction modern carbon of 1.08–1.17 (Markgraf et al., 2003), and 1.08 for ca. 1990 (Stine and Stine, 1990).

The high fraction modern carbon and equilibrium or near-equilibrium with atmospheric CO_2 of carbon dissolved in Lago Cardiel waters is perhaps notable, given that large ^{14}C reservoir effects are observed in some high Andean lakes (Geyh et al., 1999; Rissman et al., 2015). Lago Cardiel is well removed from the Andean magmatic arc and the influence of volcanic CO_2 with low ^{14}C, which is probably the main cause of high reservoir effect observed Andean lakes. Also, the Cardiel watershed is dominated by volcanic and siliclastic sedimentary rocks, although minor Cretaceous-age marine sediment containing carbonate is exposed (Ramos, 1982). Moreover, strong year-round winds probably assist in mixing the lake.

5.2. Stratigraphy and geochronology of shoreline deposits

Stratigraphic profiles described at over thirty locations,

Table 1
Carbon-14 results from Lago Cardiel.

sample no. Car10-	lab no. AA-	material	°S	°W	height above 1988 lake	$\delta^{13}C$ PDB	$\delta^{18}O$ PDB	fraction modern C	^{14}C yr BP	±	cal yr BP	±	comments
5	93571	modern algae	−71.07082143	−48.86420068	4.5	−18.5		1.1325			post-bomb		2010 beach
5	93572	modern organic	−71.07082143	−48.86420068	4.5	−29.4		1.0251			post-bomb		2010 beach
5	95644	tufa	−71.07082143	−48.86420068	4.5	4.7	−2.6		1980	20	1930	50	along modern shoreline
7	95144	tufa inner	−71.07013446	−48.86374522	5.1	4.9	−1.5		5820	30	6630	100	
7	95645	tufa outer	−71.07013446	−48.86374522	5.1	4.2	−2.2		2660	20	2770	20	
8	104448	shell, *Chilinia*	−71.07013446	−48.86374522	5.9	−0.1		1.167					bottle glass associated
10	95464	tufa inner	−71.06686994	−48.86294922	7.7	4.3	−1.0		8480	40	9500	40	reworked?
10	95729	Car10 inner (white)	−71.06686994	−48.86294922	7.7	4.9			4990	30	5710	120	reworked?
10	95728	Car10 inner (gray)	−71.06686994	−48.86294922	7.7	4.6			9110	50	10260	110	reworked?
10	95647	tufa outer	−71.06686994	−48.86294922	7.7	5.8	−2.3		2870	20	2990	70	
11	96381	tufa (thin) coat	−71.06686994	−48.86294922	7.7	7.1	−3.4	1.078					
14	92041	shell, *Chilinia*	−71.05788819	−48.85972749	20.4	0.5			4550	50	5170	200	Ventoso shoreline
15	93573	shell-reworked	−71.0591599	−48.85217457	20.5	2.4			9790	40	11220	40	Ventoso shoreline, reworked
16	95648	tufa-reworked	−71.0591599	−48.85217457	21.5	3.8	−2.3		35040	1040			Ventoso shoreline, reworked
19	93093	shell, *Chilinia*	−71.07828108	−48.95303318	35.7	0.7			6360	40	7300	90	
21	93094	shell, *Chilinia*	−71.07915705	−48.95537444	38.5	0.0			6490	40	7390	80	
22	93574	shell, high spire	−71.0573662	−48.95599987	67.4	1.3			40,920	260	44460	580	profile in Cerro Goro Shoreline
22	93575	shell, Lymnaied	−71.0573662	−48.95599987	67.4	0.0			36,000	210	40650	540	profile in Cerro Goro Shoreline
23	93576	carbonate coats	−71.0573662	−48.95599987	67.4	3.6			27,040	110	31070	190	post-Cerro Goro soil cement
30−1	104449	shell reworked	−71.369669	−48.8539877	4.5	2.0			1760	30	1660	90	reworked in modern shoreline
30−2	104450	shell reworked	−71.369669	−48.8539877	4.5	−1.4			3340	40	3580	90	reworked in modern shoreline
34a	95023	shell, *Chilinia*	−71.05659671	−48.95755201	55.0	−4.8	0.1		9920	50	11330	140	transgression to the Cardiel shoreline
36b/c	95023	shell, *Chilinia*	−71.05423094	−48.9578	55.9	−6.4			9810	20	11230	20	back bar to the Cardiel shoreline
37a	95024	shell, *Chilinia*	−71.05997011	−48.95752768	57.8	0.2	−1.7		9330	50	10540	150	top of Cardiel shoreline
40b	95025	shell, *Chilinia*	−71.06906133	−48.95767952	42.1	0.6	−2.0		8950	50	10060	160	regression from Cardiel shoreline
41	93095	shell, *Chilinia*	−71.07225441	−48.95791897	41.2	−0.2			8660	40	9610	80	regression from Cardiel shoreline
42a	93096	shell, *Chilinia*	−71.07378808	−48.95767543	42.1	1.8			8260	40	9250	150	base Cardiel regression
42b	93569	shell, *Chilinia*	−71.07378808	−48.95767543	43.1	−0.8			8290	40	9310	140	top of Cardiel regression
43	95026	shell, *Chilinia*	−71.07863905	−48.95605853	33.9	−0.4	−1.8		6440	40	7360	70	regression from Cardiel shoreline
44	95649	shell, *Chilinia*	−71.08769449	−48.95241301	22.9	1.9	−1.8		4550	30	5160	130	back bar to Ventoso shoreline
46	95027	shell, *Chilinia*	−71.05116105	−48.84025296	54.1	0.4	−2.0		9010	50	10200	160	shell in well-defined shoreline
49a	95029	shell, *Chilinia*	−71.0385049	−48.90012525	54.1	−0.9	−1.9		9130	50	10290	110	in Cardiel shoreline
49b	95030	shell, *Chilinia*	−71.0385049	−48.90012525	56.8	1.4	−1.8		9420	50	10650	130	in Cardiel shoreline
50a	95031	shell, *Chilinia*	−71.1617007	−49.02810205	30.2	−3.3	−2.3		8050	40	8950	130	
50b	95146	inner tufa coat	−71.1617007	−49.02810205	30.2	4.2	−2.4		9710	50	11150	190	reworked
50b	95652	outer tufa coat	−71.1617007	−49.02810205	30.2	6.8	−3.6		5920	30	6740	70	
50c	96467	inner tufa in float	−71.1617007	−49.02810205	31.1	4.0			8160	40	9100	120	
50c	96469	outertufa in float	−71.1617007	−49.02810205	32.1	4.0			8810	40	9850	230	
51a	95032	shell, *Chilinia*	−71.16128391	−49.02858669	38.5	−1.2	−2.1		8110	40	9050	80	
51b	95635	tufa in float	−71.16128391	−49.02858669	38.5	3.9	−2.3		33390	840			reworked tufa
52	95834	tufa plate inner	−71.16816557	−49.01757156	8.2	4.5	−1.7		5610	40	6380	80	
52	95640	tufa plate middle	−71.16816557	−49.01757156	8.2	4.3	−2.4		5900	30	6720	60	
52	95639	tufa plate outer	−71.16816557	−49.01757156	8.2	4.8	−1.0		2500	20	2580	120	
52h	95837	tufa head inner	−71.16816557	−49.01757156	8.2	4.6	−1.2		1210	30	1130	90	
52c	96730	tufa inner	−71.16816557	−49.01757156	8.2	4.0			16420	110	19810	260	
52c	96466	tufa middle	−71.16816557	−49.01757156	9.1	−1.7			5250	30	6000	130	
52c	95641	tufa inner	−71.16816557	−49.01757156	8.2	3.9	−3.1		17540	120	21200	370	
52c	95642	tufa outer	−71.16816557	−49.01757156	8.2	4.4	−2.6		2570	20	2740	20	
53	95145	tufa coat on rock	−71.1676517	−49.01991133	10.0	4.4	−2.6		2560	30	2720	130	
55	95150	tufa plate	−71.16484618	−49.02303191	11.9	4.6	−1.9		610	20	600	50	
55	95650	tufa fracture coating	−71.16484618	−49.02303191	11.9	4.4	−2.4		2360	20	2360	50	
56	95651	shell	−71.16484618	−49.02303191	9.1	0.1	−2.4	1.18					
57a	95033	shell	−71.24289714	−49.03934184	32.1	−1.2	−1.5		6400	30	7340	70	
57b	95835	plants fragments	−71.24289714	−49.03934184	32.1	−23.9		1.1059					secondary roots?
58	95141	shell	−71.24343326	−49.04426148	54.1	0.2	−1.6		8950	40	10070	80	
60	95840	shell	−71.24738536	−49.04662245	51.3	0.8	−2.0		9600	50	10940	200	

combined with ~30 new ^{14}C dates (Table 1; Fig. 4) from aquatic shell, ranging in age from 40, 920 ^{14}C yrs B.P. to post-bomb, provide the main basis for our lake-level history. The stratigraphic sequence is presented here chronologically, involving three major transgressive-regressive lake cycles that led to the formation of three conspicuous shoreline complexes: the Cerro Goro (oldest), Cardiel, and Ventoso (youngest).

We obtained an additional ~25 ^{14}C dates on a number of pre-modern tufa samples, ranging from 1 to 4 dates/sample, depending on the number of layers present. The resulting ages span a wide range, from 35,040 ^{14}C yrs B.P. to post-bomb (Table 1). All but one of the results (Table 1; Car10-50c) follows the expected stratigraphic

order, with the oldest dates in the interior of the tufa and the youngest on the outside. The tufa dates supply vital information on those times when the lake was at or just above the modern level. Importantly, our dataset reveals several clear instances in which older shell and tufa were reworked (Fig. 6a) downslope during later lake phases, and incorporated into younger deposits.

5.2.1. >40 ka: the Cerro Gorro (+72–75 ml) shoreline highstand

The highest (+72–75 m) unequivocal shoreline in the basin is the Cerro Goro shoreline, which formed sometime >40 ka. The lacustrine deposits associated with highest, Cerro Goro shoreline complex consist mainly of coarse, lithic-rich sand and well-rounded fine to medium pebbles, in places organized into well-imbricated beach shingles. Thickness is at least 5 m, as described in sections Car10-22/23 at the top of the Rio Cerro Goro transect (Fig. 2a, c, 4a).

Shell is very rare in these deposits and was found at only one location (Fig. 4a; Car10-22/23). Two shells returned uncalibrated ages of 40,920 ± 260 and 36,000 ± 210 ^{14}C yrs B.P. These ages are at or near the limit of ^{14}C dating for shell carbonate, which generally contaminate more easily than charcoal and organic matter. ^{14}C ages in the 40–35 ka range are common in deposits known to be »50 ka (Rech et al., 2011), requiring only 1–2% modern contamination by modern carbon to yield a much younger apparent ages for »50 ka shell samples. A sample of soil carbonate coating beach gravels in this section returned an uncalibrated ^{14}C date of 27,040 ± 110 ^{14}C yrs B.P. (Table 1; Car10-23). As this carbonate is post-lake, it provides a minimum age for the shoreline, in support of the shell dates.

An age >40 ka for the Cerro Goro shoreline complex is suggested by other evidence as well. It is heavily dissected, with much higher gullying density than the next youngest shorelines at ~+54–58 m (Stine and Stine, 1990). Soil development is also strong in capping soils, attaining Stage I-II (*sensu* Gile et al., 1966) for the carbonate horizons, compared to weak Stage I in soils capping the younger shorelines.

Further evidence of older, >30 ka lake cycles comes from fragments of old tufa reworked into the younger Holocene lake deposits found in two locations. In both instances (Table 1: Car10-16, +21 m, and Car10-51b, +38 m), the tufa yielded ^{14}C ages >30 ka. This indicates that tufa from a >30 ka lake cycle was widely available for reworking by the Holocene-age lake. Better determination of the age of the Cerro Goro shoreline and other possible older lake cycles awaits further research, but all current evidence indicates the shoreline formed >40 ka.

5.2.2. >40–11.6 ka: lower lake levels

During the period 40–11.6 ka, the lake was close to or below the level of the modern lake, inasmuch as no substantial deposits and only two dates from a single low-elevation tufa have been identified by us from this period. The dated tufa (Table 1 and Fig. 4a: Car10-52c) from +8 m displays several distinct layers. Two samples from the innermost layer yielded dates of 19,810 ± 260 and 21,200 ± 370 B.P (Fig. 3a), indicating a lake was present just above the modern level, at least briefly at these two times.

5.2.3. 11.3 to 10.1 ka: highstand at the Cardiel (+54–58 m) shoreline complex

Lago Cardiel was at its highest level in the last 40 ka when it formed at least three closely spaced shorelines between +54 and 58 m, composing the Cardiel shoreline complex that dates to 11.3 to 10.1 ka. The deposits underlying the shorelines are continuously exposed downslope well below +54 m and represent a single lake cycle as the lake transgressed to and regressed from the Cardiel shoreline complex (Fig. 5a). We obtained seven dates (Table 1: Car10-34a, 36b/c, −37a, −46, −49a, −49b, 60) on shell from the high shoreline complex above +54 m at three different basin locations that range from 11,330 ± 140 (Table 1, Car10-34a) to 10,070 ± 80 B.P. (Car10-58). This marks the duration of the highest stand of the lake in the last >30 ka (Fig. 6). The 11,330 ± 140 B.P. date comes from shell at ~56 m (Table 1 and Fig. 5a, Car10-34a) in lacustrine gravels that mark the transgression of the lake through this elevation. A stable shoreline and back-bar complex along the Cardiel Shoreline appears to have developed by 11,230 ± 20 (Table 1, Car10-36b/c), based on a shell date from Section 36 (see topographic profile along top of Fig. 4a) in back-bar deposits.

5.2.4. 10.1–5.1 ka: high but falling lake levels

Our evidence indicates that the lake gradually contracted below the high Cardiel shoreline complex, but fluctuated considerably during the period 10.1–5.1 ka. The lake appears to have been lower between 8.9 and 7.5 ka and perhaps slightly lower 6.7–5.8 ka, and experienced increases centered on ~7.4 ka (no clear shoreline associated) and 5.2 ka (the Ventoso Shoreline) (Fig. 6a).

The regression of the lake from the high Cardiel shoreline is readily traceable around the lake perimeter as a semi-continuous beach of shingle gravel and sand, rich in shell, that is cut into pre-lake alluvium down to an elevation of +30 m (Fig. 5a). The start of the lake level decline is defined by a shell date of 10,060 ± 160 B.P. (Table 1: Car10-40b) from the top of profile Car10-40 (Fig. 5a). Four additional shell dates (Table 1: 42a, 42b, 50a, −58) from these deposits at Cerro Goro and Cañon Último trace the gradual regression of the lake between 10.1 and 8.9 ka by ~25 m to +30 m. The lake appears to have further dropped below modern lake elevations between 8.9 and 7.5 ka, based on bracketing ages from older Cardiel and younger Ventoso highstand deposits, and supported by the total lack ^{14}C dates from this interval (however, see Stine and Stine (1990) data discussed in Section 6).

We obtained two shell dates (Table 1: Car10-19, −21) from +36 to +38 m that record a slight rebound of the lake between 7.3 and 7.4 ka. Another exposure at Cañon Último also fixes the shoreline of the lake in the +32–47 m range at 7340 ± 70 B.P. (Table 1, CAR10-57a; Figs. 2d and 4f). No clear paleoshoreline is associated with this apparently brief lake expansion, suggesting perhaps that it did not stabilize at a single elevation for very long.

For the interval 6.7–6.0 ka we obtained four dates from near Estancia Primero Argentino (Fig. 2a, d) on tufa (Table 1: Car10-50b, −52ai, −52-am, −52c) in the +8 to +30 m elevation range. These dates therefore appear to indicate a modest decline in the lake, but see also section 6 of this paper.

The last major rise of the lake during the Holocene is marked by the Ventoso shoreline, the best preserved of the prominent paleoshorelines in the basin. The crest of the Ventoso shoreline typically lies in the +21–22 m range. The beach berm is 2–3 m tall, has steep banks, and is relatively uneroded compared to older, higher elevation shorelines. Unlike the Cerro Goro and Cardiel, the Ventoso shoreline is also marked by a sharp transition in modern plant cover: above it the landscape is well vegetated and lacustrine deposits are mantled with slope wash and secondary soil development, whereas below it plants are very scattered and lake deposits are widely exposed.

Deep gullies expose >2 m of the Ventoso shoreline deposits at three localities, which contain abundant shell and tufa. Car10-14 in the NE Cardiel area (Figs. 1 and 5b) is the most complete, where shoreline deposits composed of basal gravel mixed with some reworked tufa rest disconformably on older lacustrine silt. A shell-rich sand overlies the basal gravel, and the whole sequence is draped with a 10-30 cm-thick layer of well-polished, imbricated gravels. Exposures at Car10-15 (near Car10-14, Fig. 5b) and Car10-44 (from Cerro Goro, Fig. 5a) also expose the basal gravel and shell-rich sand of this lake cycle.

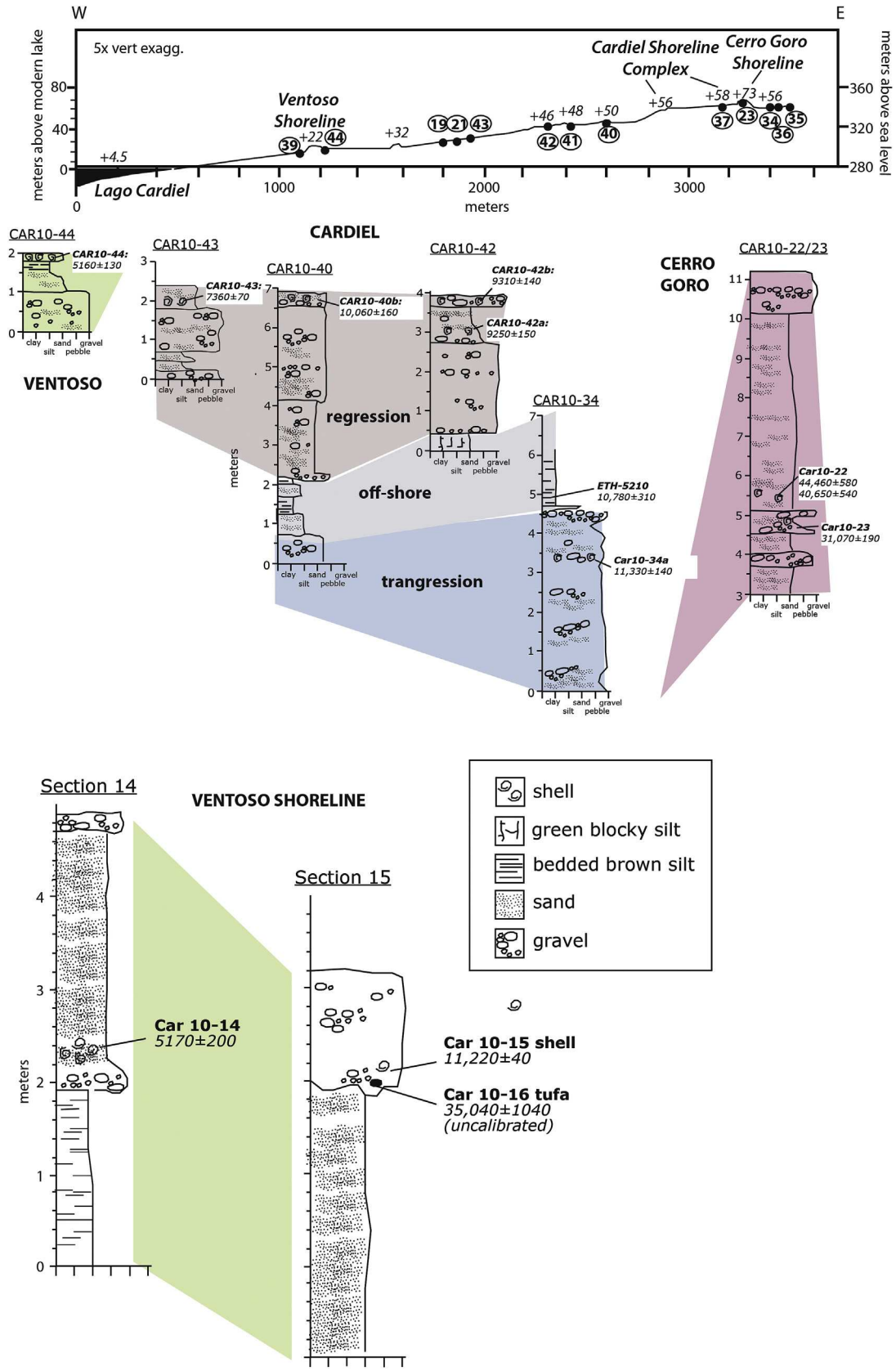

Fig. 5. a) Topographic cross-sections along Arroyo Cerro Goro (see Fig. 2c location of profile and sections) showing key stratigraphic sections (circled numbers) in relation to the major shoreline complexes and their elevations relative to the 1988 lake level in italics, with representative stratigraphic sections tied to the topographic profile above; b), two stratigraphic profiles from the NE sampling area (see Fig. 2b for location of sections). CAR10-34 is in a stratigraphically inset position below the older Cerro Goro shoreline. All dates are expressed in cal yr BP; see Fig. 5b for legend.

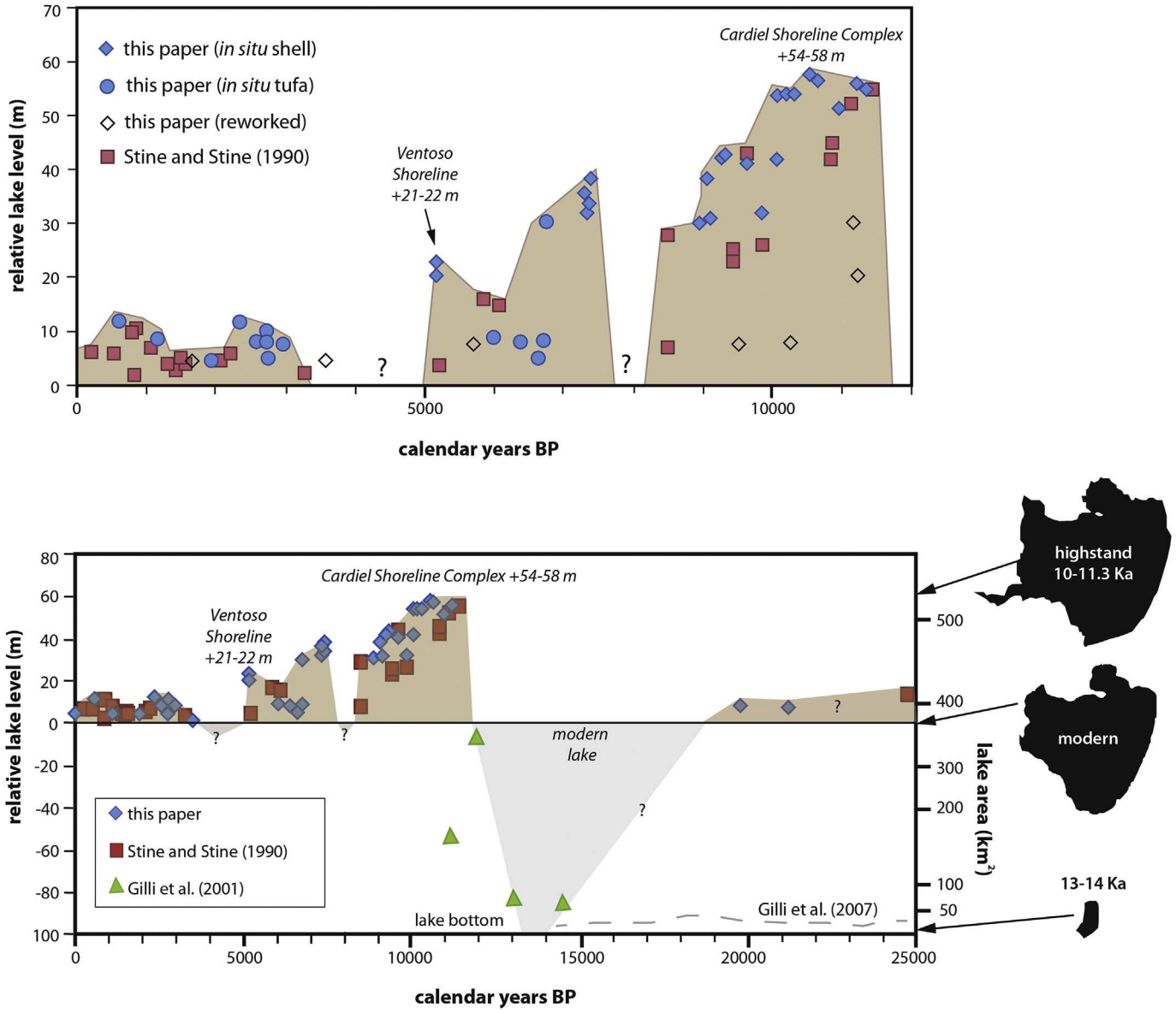

Fig. 6. Reconstructed changes in Lago Cardiel showing calendar ages of samples versus relative lake level on left a) spanning the last 12,000 cal yrs, from this study (diamonds and circles) and that of Stine and Stine (1990) (squares). Main shorelines and interpreted lake level curve (brown) also shown; b), spanning the last 25,000 cal yrs, with the addition of lake area on right and sub-modern lake level samples from Gilli et al. (2001) (triangles). An alternative view of the lake level history prior to ~13 ka as discussed in Gilli et al. (2007) is shown as a dashed gray line. Reconstructed lake levels above modern in brown and below modern in gray. (For interpretation of the references to colour in this figure legend, the reader is referred to the web version of this article.)

Four ^{14}C dates from shell and one from tufa were obtained along the Ventoso shoreline. Shell in the beach sands 30–90 cm above the basal gravel from sections Car10-14 and −44 returned nearly identical dates of 5170 ± 200 (Table 1: Car10-14) and 5160 ± 130 B.P. (Car10-44). At section Car10-15 (Fig. 5b), abraded shell and chunks of tufa, both from the basal gravel, returned dates of 11,220 ± 40 (Table 1; Car10-15) and an uncalibrated 35,040 ± 1040 B.P. (Car10-16), respectively. The abraded shell and tufa debris are likely both reworked from older lake deposits, whereas the shell dates of 5160–5170 B.P. can be taken as primary and unreworked.

Combining all this information, we interpret the record to show that the lake began to rise from the slight dip at 6000 B.P. in lake level to ~+15 m, reaching the Ventoso (+21–22 m) shoreline by at least 5170 B.P. However, the full duration of lake level at the Ventoso shoreline remains unknown.

5.2.5. 5.0–3.0 ka lower lake level

There is a second conspicuous dating gap in our record from about 5.0 to 3.0 ka, suggesting either inadequate sampling, or more likely a rapid drop after ~5100 B.P to levels below the current lake. Based on our evidence, the lake rebounded by no later than ~3.0 ka (Table 1, Car10-10).

5.2.6. 3.0 ka to historic period: moderate lake levels

Our evidence for this period, drawn entirely from nine ^{14}C dates on tufa, shows that a shallow (<+17 m) and variable lake was present from 3.0 ka to the historic period (Fig. 6). At least two minor increases in lake level are represented during this interval by single tufa ages at 2.4 and 0.6 ka.

5.2.7. Historic shorelines

We made several observations that allow us to constrain lake-

level changes in historic times to <~+9 m. One is the identification of abraded bottle glass along a distinct shoreline berm at +8.5 m at two locations (Fig. 2b, d: Car10-10.5, −56), ~3.5 m above the 2010 lake level. This elevation also marks a distinct break in rock surface color and tufa type. Above this elevation, rock surfaces are darker in appearance and the tufa weathered. Below it, basalt clasts are everywhere thinly coated with fresh tufa. These yielded fmc = 1.078 (Fig. 4c and Table 1: Car10-11), indicating a post-1950 age. Hence, the lake appears to have reached +8.5 m, 3.5 m higher than in 2010, sometime since 1950.

5.3. Evaluating the shorelines above +75 m from the Tres Lagunas Valley

A low sill at ~454 masl (~180 m above the 1988 lake) divides the Cardiel Basin from the Rio Chico drainage to the east (Fig. 2). It is across this sill (referred to as the Tres Lagunas area; Fig. 2a) that Wenzens (2005) concluded that the Rio Chico once flowed, contributing to lakes in the Cardiel Basin. Wenzens (2005) inferred that the Rio Chico received significant input from Andean glaciers in the past, and so he correlated glacial recessions in the Andes with deep lakes and associated paleo-shorelines in the Cardiel basin, suggesting large meltwater input raised lake levels. In addition to the shorelines already described, Wenzens (2005) identified two even higher shorelines at +134 and + 175 m, which cut through the Tres Lagunas area. As far as we know, these shorelines appear to have been identified based only on lineaments visible in areal imagery, and they remain undated radiometrically. Wenzens (2005) assigned late Pleistocene ages to the shorelines by correlating them with glacial meltwater pulses, a view challenged by Gilli et al. (2007).

We conducted a survey of the Tres Lagunas area, described the stratigraphy in several sediment exposures, and attempted to trace the putative +134 m shoreline feature suggested by Wenzens (2005) on foot. Two gravel pits below the drainage divide (Car10-48-1 (S°48.8478, W°70.6190) and Car10-48-2 (S°48.8633; W°70.7000)) expose ~2 m of stacked paleosols. The paleosols overprint sediment that is composed of subangular gravels within local alluvial fan sediments mixed with eolian sand. Paleosols in both pits show Stage III carbonate (Gile et al., 1966), and ~20 cm thick eolian caps. Studies of comparably mature paleosols elsewhere in the region would indicate that the Tres Lagunas surface is > 100 ka old and stable (Bockheim and Douglass, 2006; Douglass and Bockheim, 2006). There is no evidence in either pit of deposition by a large river or in a lake.

The +134 m “paleoshoreline” of Wenzen (2005) appears as a lineament on the north and south sides of the Tres Lagunas valley. The lineaments mark the local truncation of older cemented alluvial gravels, and the lineaments decrease in elevation on either side of the drainage divide. Along this lineament we did not find any of the distinctive features that characterize paleoshorelines in the Cardiel Basin, such well-sorted shoreline gravels, beach sands, fossils snails, and tufas. The uneven elevation also argues against a shoreline association. Instead, these lineaments, because of the way they truncate outcrops of older alluvial gravels, appear to mark fault traces. Based on the combined field evidence, we question the existence of shorelines discussed by Wenzens (2005) above the Cerro Goro (+73–75 m) shoreline.

6. Synthesis and summary of lake-level history

We merge our results with those of Stine and Stine (1990), Markgraf et al. (2003), Gilli et al. (2001, 2005a, b) to create a composite lake level curve for past 25 ka, shown in Fig. 6b as a shaded zone superimposed on the data points from most of these sources. The lake core and geophysically based evidence are especially useful for establishing changes in lake level below the surface of the modern lake. However, these studies entail some geochronologic challenges where reliant on fine-grained carbonate and organic matter for dating. Both phases, but especially organic matter, are prone to inheritance of older carbon. Deep-lake sediments at Cardiel are clayey and low in organic matter in part due to the arid climate. Older, often non-lake organic matter can be complexed with the clays, making ^{14}C dates on bulk organic carbon, and humin and humic phases, too old, like those reported by Gilli et al. (2005b). Inheritance of old organic matter is a common and well-documented problem in high-latitude, low-productivity arid lakes such as Cardiel (Abbot and Stafford, 1996; McGeehin et al., 2004). In our summary of lake level history (Fig. 6b), we therefore focus on age controls provided only by macroscopic carbonates, wood, and aquatic plants (our results, Stine and Stine, 1990; Gilli et al., 2001, 2005a; Markgraf et al., 2003).

Our results generally verify but differ in some of the details from the original lake level history of Stine and Stine (1990) and Markgraf et al. (2003). Our work and that of Stine and Stine (1990) agree that the deeply eroded Cerro Goro Shoreline Complex is > 40 ka, and it awaits dating by other methods such as OSL. Merged records show that the period >40 to 11.5 ka probably witnessed the lowest lake levels within the range of ^{14}C dating. Neither shoreline studies obtained any dates from the 40–24 and 20–11.5 ka range, suggesting that the lake was below modern lake levels. Three dates, all from tufa (Table 1: Car10-52c; LDGO-1714b from Table 1 in Stine and Stine, 1990), suggest that the lake was at or slightly above the modern lake elevation between 20 and 24 ka. Evidence from cores for lake levels well below the modern lake during the LGM (Sequence IV discussed in Gilli et al., 2007; and see Fig. 6b) are not entirely supported by these shoreline results; however, evidence from cores partly hinges on the problematic dating of low-carbon sediments, as discussed above. A much more comprehensive effort to date tufas at or near the modern shoreline, and Sequence IV associated with the late Pleistocene lowstand should help resolve the disagreement between core and shoreline-base evidence.

Gilli et al. (2001) obtained four ^{14}C dates from cores on wood and *Ruppia* that provide key constraints on lake level for the period 20–11.5 ka (Fig. 6b). They show that the lake was 83 m below the 1988 lake level at 14,470 ± 540 B.P., and rose thereafter, reaching 53 m below the 1988 lake level by 11,150 ± 360 B.P. This last date overlaps with the oldest ^{14}C dates on the Cardiel shoreline complex (Table 1) at +54–58 m, meaning that the lake rose ~120 m and expanded in area from roughly 50–120% of modern within a few hundred years.

Our data and those of Stine and Stine (1990) generally agree in placing the lake at or near the Cardiel highstand between 11.3 and 8.9 ka, although our data are more continuous and show that the peak highstand period ends around 10.5 ka, and the lake slowly declined thereafter. The interval 10.2–7 ka is also recognized by Markgraf et al. (2003) as a period of moderate to deep-lake conditions, based on a variety of semi-quantitative proxies preserved in cores. Several tufa dates from low elevations during this time interval (e.g. Table 1: Car10-10 (inner)) are interpreted as fragments reworked downslope sometime later in the Holocene.

The highstand period ending ~8.9 ka is followed by a gap in our record between 8.9 and 7.4 ka, pointing to a period of reduced lake level. However, the gap is narrowed with two samples from Stine and Stine (1990) at around at 8.5 ka. An elevated but variable lake level from 7.4 to 5.1 ka is visible in both records.

The periods 8.5–7.5 and 5.0–3.3 ka are conspicuous gaps in the shoreline and delta records, but the combined evidence shows that the lake probably did not drop significantly below modern lake

levels at these times. Markgraf et al. (2003) note that no part of the Holocene core record stands out as markedly dry, and they depict a shallow, fluctuating lake during the mid-to late Holocene. Evidence from seismic imaging agrees with this. Sequences I-III apparently spanning the entire Holocene (since Late Glacial ACR time) blanket most of the lake bottom right up to the modern lake level (Gilli et al., 2001, 2005a,b; Ariztegui et al., 2009). Evidence from shorelines and deltas also agree with Markgraf et al. (2003) in reconstructing a similar-to-modern lake over the last 3300 years.

7. Lake area and ice volume changes, and the southern hemispheric westerlies and temperature

In this section we explore the potential linkages between the Lago Cardiel record and a number of regional and larger-scale phenomena. We begin by noting that the balance between mean annual precipitation versus evaporation/evapotranspiration determine the surface area of closed lakes, including Lago Cardiel. Lake area determines rates of moisture losses through evaporation, and in a closed basin at steady state, evaporation plus evapotranspiration must equal precipitation. We have converted lake-surface elevation to lake-surface area in Fig. 6b using our maps and reconstructions of submerged shorelines discussed in Gilli et al. (2005a). This shows how significantly lake-surface area, and thus moisture balance, must have changed in the past. For example, the lake was almost completely dry by 13 ka, whereas by 11.3 ka, lake area had increased to it hydrologic maximum of 136% of modern. During most of the Holocene, the lake appears to have remained within 90–110% of modern. It is beyond the scope of this paper to quantify these paleohydrological changes through hydrologic modeling, but the changes are so large that we can discuss their probable causes in terms of modern climate. One point that is clear is that temperature changes alone cannot have caused the observed lake-level changes. Holding precipitation constant, colder global temperatures and lower evaporation rates 30–11.5 ka should have increased lake sizes, whereas warmer Holocene temperatures, especially in the early to mid-Holocene, would have reduced them. Instead we observe the opposite pattern of lake response, where a deep and expansive lake persisted throughout the warmest period of the early Holocene (Moreno and Videla, 2016; Villa-Martínez et al., 2012). If anything, even greater increases in precipitation and/or wind speed decrease are required to offset the effects of generally warmer Holocene temperatures over the southern Andes. So, we must invoke causes other than temperature, such as wind stress (as it effects evaporation rates) or changes in precipitation linked with atmospheric circulation, as the main control on lake area variations.

We invoke the modern E-W precipitation pattern to explain our findings. In the context of the dipolar relationship of precipitation on either side of the Andes described previously, this means that periods of weaker SHW result in less precipitation in the western Andes, but enhanced precipitation and less wind on the east side, thus increasing the size of Lago Cardiel (Fig. 7). In this view, low-lake periods such as 20–11.5 ka would coincide with times when the SHW were strongest and/or had a mean or focused position at the latitudes near (e.g. 49–53°S) Lago Cardiel. High lake periods such as 11.3 ka to 8.9 ka represent times when the SHW were weakest and its core of fastest winds was to the south of Lago Cardiel. We can merge evidence from Lago Cardiel with other records in the region (Table 2) to reconstruct changes in the mean position of the SHW over the past 25 ka (Fig. 7). The reconstruction is more speculative or incomplete for some time periods than others, such as the deglacial period 18–11.3 ka, when the stratigraphic record is submerged at Cardiel but large changes in climate such as the Younger Dryas (YD), Antarctic Cold Reversal (ACR), and several Heinrich Events (HE) are known to occur. In this synthesis we mainly interpret the Cardiel record in terms of mean or core SHW position, but recognize that the record can also be interpreted in terms of wind strength, which seasonally is closely tied to position and wind-belt width (Lamy et al., 2010; Villa-Martínez et al., 2012; Kohfeld et al., 2013). Also, the westerlies represent a boundary between warmer and colder air masses to the north and south, respectively. We present Figure 8 as a speculative but testable hypothesis relating lake level to SHW position and/or strength and associated climates. There is certainly considerable general justification for linking the Lago Cardiel lake-level record to the changing position of the SHW (Fig. 8), as already pointed out by Moreno et al. (2010) and Fletcher and Moreno (2011). Most (e.g. Heusser, 1989; Moreno et al., 1999, 2012; Lamy et al., 1999, 2010; Stuut and Lamy, 2004, Anderson et al., 2009; Villa-Martinez et al., 2012), but not all e.g. Markgraf et al. (1992) studies agree with the general direction of changes in the position of the SHW shown in Figure 8. Other records from east of the Andes such as from Lago Potrok Aike (Haberzettl et al., 2007, 2008; but see also Wille et al., 2007) generally follow that of Lago Cardiel. By contrast, many records west of the Andes show the opposite pattern to Cardiel and Potrok Aike (Fig. 1), consistent with the modern east-west climate dipole (Fig. 7). For example, other phenomena such as glacial extent in the Andes during the Holocene can be predicted to mirror reasonably well the Cardiel lake size. Holocene temperature variations were relatively small, but times of strong westerlies at the latitude of Lago Cardiel should have been accompanied by growth of ice volume in the Andes, but by decreases in lake size east of the Andes (Fig. 6).

A final connection to our records and hypothesized SHW history (Fig. 8) recognizes the following points. First, air and sea-surface temperature, amplified by feedbacks, control the position and intensity of major wind belts, such as the SHW and those tied to the Antarctic Polar Current (ACC) (Hodell et al., 2001; Anderson et al., 2009; Lamy et al., 2010). For example, global climate modeling (Timmermann et al., 2007) and observations (Thompson and Soloman, 2002; Chen and Held, 2007; IPCC, 2013) in recent decades show that SHW have shifted poleward in response to rising global temperature. A range of studies, drawing on evidence for sea-ice extent, and biological, sedimentologic, and paleotemperature indicators, conclude the ACC and SHW shifted northward during glacial periods (e.g. Hays et al., 1976; Habbeln et al., 2002; Mohtadi and Habbeln, 2004; Kaiser et al., 2005; Govin et al., 2009; Gersonde et al., 2005). Consequently, in Patagonia, the shifting of the core of the SHW, as shown by the dashed line on Figure 8, is also associated with a latitudinal shift in air characteristics, including temperature and precipitation (e.g., 1σ line on Fig. 8) (Garreaud, 2007; Moreno et al., 2010).

In this last part of our discussion we merge evidence for each time period from Lago Cardiel with other records in the region to reconstruct changes in the SHW over the past 25 ka (Fig. 8), in glacial (Fig. 9g) and sea ice extent (Fig. 9f), and in southern hemispheric ocean (Fig. 9c) and air (Fig. 9d) temperatures.

24–20 ka: Lago Cardiel was at about the modern level from 24 to 20 ka. We speculate that this is the result of reduced evaporation due to colder temperatures, countered by stronger winter westerlies. Consistent with this, a variety of records from the western Andes and Pacific Coast <50- 33°S (e.g. Moreno et al., 1999, 2010; Moreno and Leon, 2003; Markgraf et al., 2007; Fletcher and Moreno, 2011) show wetter conditions than today, with generally cold and dry conditions south of ~50°S (Markgraf and Uber, 2010). This pattern is interpreted by most of these researchers to reflect a broader and more northerly position of the westerlies during this time period (Fig. 8) under very cold full-glacial conditions. Colder temperatures, and secondarily, more precipitation (at least west of

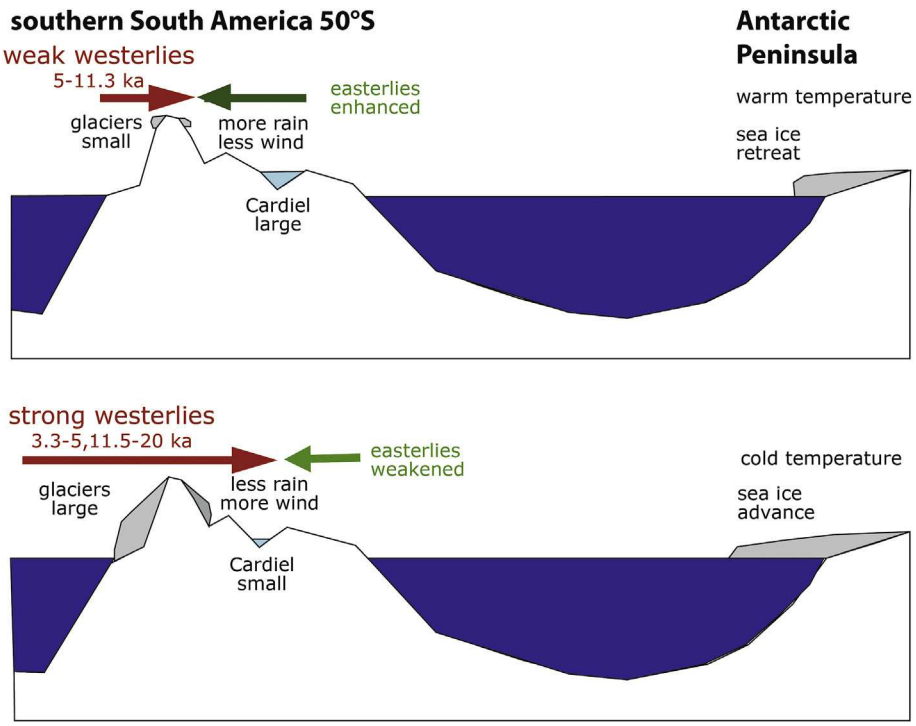

Fig. 7. Conceptual diagram illustrating the response between the strength of the Southern Hemispheric Westerlies (SHW) at the latitudes of southern Patagonia (e.g, 50°S) and: precipitation, continental glaciers, and lakes in South America ~50°S, and Antarctic air temperatures and sea-ice.

Table 2
Main references used to reconstruct southern hemispheric westerlies changes.

reference	lat °S	long °W	type	notes
Anderson et al. (2009)	various		marine opal flux	ACR and westerlies shifts 2–28 ka
Fletcher & Moreno (2011)	various		various	shifts and intensity changes 0–14 ka
Garcia et al. (2012)	51		glacial	Late-glacial ice changes
Hall et al. (2013)	54–55	69–70	glacial	deglacial ice retreat and warming
Hebbeln et al. (2002)	~33	72	various marine	paleoproductivity changes 0–33 ka
Heusser (2003)	various		pollen	overview of vegetation and westerlies shifts
Jenny et al. (2003)	34	71	lacustrine	Holocene westerlies shifts
Lamy et al. (1999)	33	72	marine clays	shifts in weathering intensity 0-28ka
Lamy et al. (2004)	41	74.5	marine clays	shifts in weathering intensity 8-28ka
Lamy et al. (2010)	various		various	shifts and intensity changes 0–12.5 ka
Markgraf and Uber (2010)	52–54	67	pollen	vegetation changes and the westerlies
Moreno et al. (2009)	50–51	72–73	glacial + pollen	deglacial Antarctic Polar front shift 9–12.5 ka
Moreno et al. (2010)	various		pollen	shifts and intensity changes 0–13 ka
Moreno et al. (2015)	40–43	72–74	pollen + glacial	deglacial warming and ice retreat

the Andes), also led to extensive glacial expansion during this time along the Pacific slope of the southern Andes (Denton et al., 1999; Kaplan et al., 2008).

20–13 ka: This period is a major stratigraphic gap in the exposed shoreline record at Lago Cardiel, and core evidence confirms that Cardiel was probably below the modern levels during most if not all of this time. This suggests that the SHW shifted southward or intensified 20–14 ka, stabilizing the mean annual core of the SHW at the latitude of the lake for some extended period. Starting with the glacial termination after ~18 ka, warm(er) conditions existed throughout the middle to high southern latitudes, especially in Patagonia (e.g. Moreno et al., 2015; Hall et al., 2013). Temperatures, however, did not reach full interglacial values right away, and this period was still colder than today in Antarctica and the southern hemisphere (Fig. 9c and d; Kaiser et al., 2005; Heusser, 2003; Anderson et al., 2009; Garcia et al., 2012), coincident with very dry conditions at Lago Cardiel, as the SHW weakened or shifted slowly southward and over the latitude of 49°S. By 13 ka, Lago Cardiel nearly dried up by dropping to its lowest levels in the entire 30 ka record, during the Antarctic Cold Reversal from 14 to 12.3 ka, the coldest time during the glacial to interglacial transition (Moreno and Videla, 2016). This is coincident with the most extensive glacial advances in the Andes (Moreno et al., 2009; Strelin et al., 2011; Garcia et al., 2012) after deglaciation.

12.5–11.5 ka: Evidence from cores indicates that Lago Cardiel expanded markedly during this time, growing in area from near 0–100% of modern. After the ACR, through the YD chron and earliest Holocene, icefield outlet glaciers (as well as smaller glaciers) in Patagonia retreated from late glacial ACR expansions to their near-present limits or even less (Strelin et al., 2014). We can interpret this in terms of a sharp increase in Antarctic sea and air temperatures that followed the end of the ACR (Fig. 9d from Ciais et al., 1992, Fig. 9c from Kaiser et al., 2005). This temperature increase weakened (Villa-Martinez et al., 2012) and/or shifted

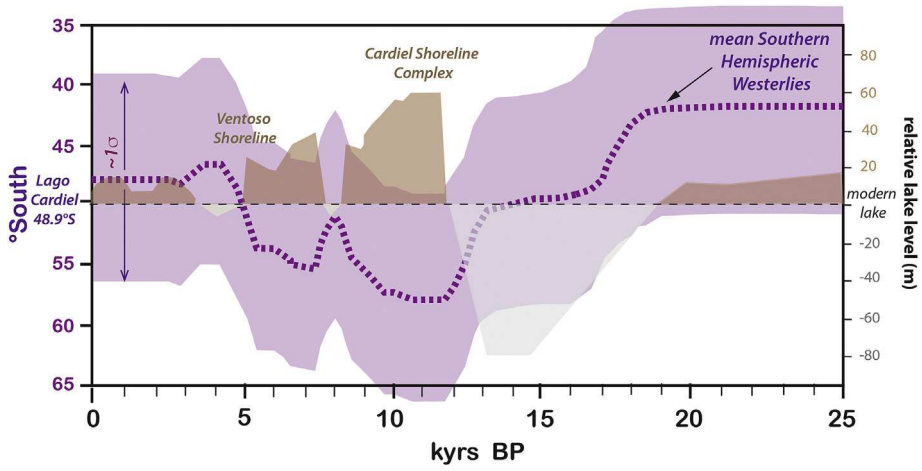

Fig. 8. Hypothesized latitudinal migration of the mean or annual position of the Southern Hemispheric westerlies (SHW) over the past 25 ka, compared to reconstructed levels of Lago Cardiel. The mean annual SHW position shown as a purple dashed line, and approximate 1σ latitudinal range of precipitation shown as purple shadow; the 1σ range is estimated from the near-normal distribution of westerly-related precipitation with latitude from western Chile, which is shown as a dashed line in Fig. 3. Lake levels above (in brown) and below (in gray) the modern lake level. (For interpretation of the references to colour in this figure legend, the reader is referred to the web version of this article.)

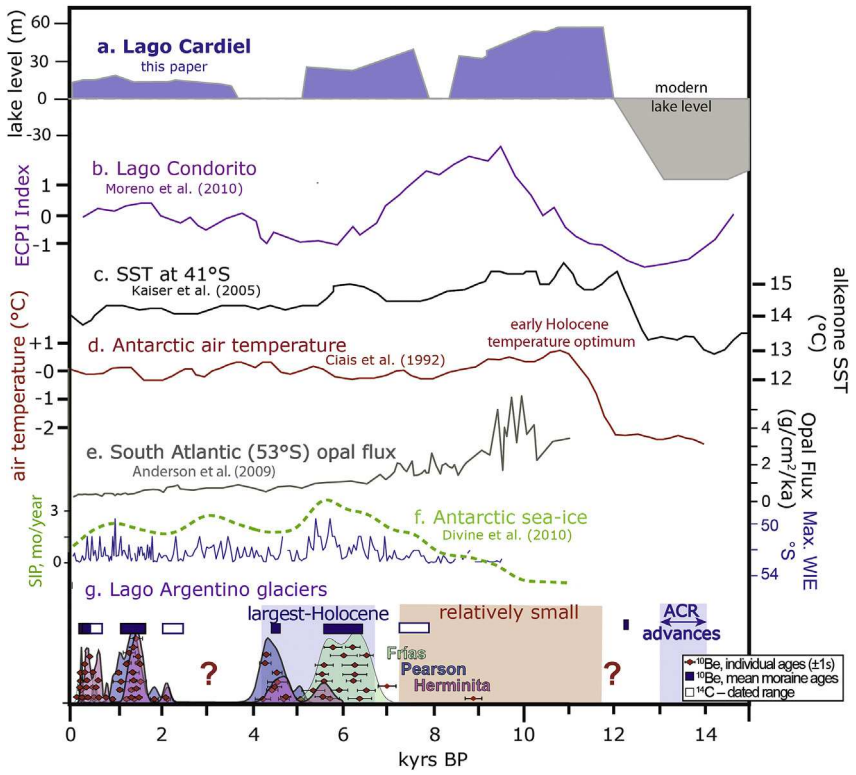

Fig. 9. Comparison of the a) reconstructed lake-level curve from Lago Cardiel to southern ocean and Antarctic records; b) pollen record from Lago Condorito from Moreno et al. (2010) at 42°S; the EPCI Index compares Valdivian rainforest trees *Eucryphia* + *Caldcluvial* north Patagonian rainforest podocarps; a high ratio indicates drier conditions, and lower ratios wet; c) alkenone-based sea-surface temperature from ODP Site 1233 at 41°S off the coast of Chile (Kaiser et al., 2005) and d) reconstructed air temperature from the average of three East Antarctic ice cores from Ciais et al. (1992), both showing the early Holocene temperature optimum; e) opal production at 53°S from Anderson et al. (2009); f) sea-ice presence (50–53°S; Divine et al., 2010): left axis sea-ice presence (SIP) in months/yr, and right axis winter ice extent (WIE) in degrees south latitude; g) the South Patagonian Icefield outlet glacier history, compiled from Strelin et al. (2014) and Kaplan et al. (2016), which is at similar latitudes to Lago Cardiel. Strelin et al. (2014) also summarizes prior studies in the region. Summed probability curves and individual ^{10}Be ages for three outlet glaciers around Lago Argentino, southern Patagonia (~49–50°S), about 100–150 km south of Lago Cardiel. The 'camel humps' in essence reflect times of moraine formation during glacier expansion. After achieving maximum extents in the mid-Holocene, since ~4400 years ago the Patagonian Icefield has generally experienced a net decrease in size during successive century-scale advances.

(Fletcher and Moreno, 2011) the core of the SHW from over Lago Cardiel ~13 ka to well south of Lago Cardiel by 11 ka (Fig. 8).

11.3–8.9 ka: Lago Cardiel remained at or near its hydrologic maximum (>120% of modern) spanning the period 11.3–8.9 ka, and correspondingly there is evidence from many records west the Andes 34–50°S for warm and dry conditions with a greater incidence of fires. The close correspondence of aridity and fire indicators from the pollen and charcoal record from Lago Condorito

(Figs. 1 and 9b; EPI index of Moreno et al., 2010) stands out. Most researchers invoke a large southward shift of the SHW to explain this period of mid- and high-latitude aridity west of the Andes (Heusser, 1989; Villagrán, 1990; Villagrán and Varela, 1990; Haberle and Bennett, 2004; Jenny et al., 2003; Moreno and León, 2003; Valero-Garcés et al., 2005; Lamy et al., 2010). The highstand at Lago Cardiel requires that this southward shift must have centered the SHW well to the south of Lago Cardiel at 49°S from 11.3 to 8.9 B.P.

The early Holocene was generally a time of reduced Patagonian ice (Strelin et al., 2014; Kaplan et al., 2016) (Fig. 9g). This glacial minimum in the Andes, and hydrologic maximum at Lago Cardiel east of the Andes, coincide with peak Antarctic air- and sea temperatures (Fig. 9d from Ciais et al., 1992, Fig. 9c from Kaiser et al., 2005; Masson et al., 2000; Hodell et al., 2001), retreat in sea-ice (Fig. 9f; Hodell et al., 2001; Divine et al., 2010; Kaplan et al., 2016), and southward shift in wind belts indicated by increased upwelling 52–63°S (Fig. 9e; Anderson et al., 2009), during the so-called Hypsithermal or Holocene Temperature Optimum (Fig. 9c and d).

8.9–5.1 ka: Generally declining but fluctuating lake levels 8.9–5.1 ka point to variable but gradually diminishing moisture balance in the lake. West of the Andes at >50°S, this period corresponds to a step-wise and gradual reduction in aridity (Fig. 9b, lower EPI index; Moreno and Leon, 2003; Jenny et al., 2003; Villa-Martínez et al., 2003). Viewed strictly in terms of the westerlies, this can be interpreted to indicate persistence of the core of the SHW south of 49°S, but with slow and variable net drift northward through the middle Holocene. Glaciers in the Andes generally were smaller than subsequent Neoglacial limits through this period, although a relatively limited glacier re-advance sometime between ~7.7 and 7.2 ka (Strelin et al., 2014) may coincide with low lake level, which preceded the brief rebound of Cardiel by 7.4 ka.

Well before 6 ka, the Hypsithermal ended in southern South America (Moreno and Videla, 2016). By 6 ka, outlets of the South Patagonian Icefield reached expanded positions, and remained so until around 4.5 ka (Fig. 9g). Before 6 ka, Antarctic sea-surface temperatures remained elevated (but declined) (Fig. 9c and d) and sea-ice was restricted (but expanding) (Fig. 9f) at first (Hodell et al., 2001; Divine et al., 2010), denoting a weaker SHW or a continuing southerly position. We conclude a gradual strengthening or northward drift of the SHW over the Patagonia-South Atlantic sector promoted major glacier expansions and greatest sea ice coverage (Mercer, 1982; Kaplan et al., 2016), in agreement with declining but fluctuating lake levels. Indeed, the decline in Cardiel level after 8 ka appears to have culminated in a relative low around 6 ka, before rising slightly to the Ventoso shoreline (Fig. 6a); during this interval Lago Argentino outlet glaciers started to expand towards their maximum Holocene positions, some of which reached such extents already by 6 ka.

5–3.3 ka: There is a clear stratigraphic gap in the exposed shoreline record, probably due to sub-modern lake levels. Viewed in terms of westerlies position, this suggests that the core of the SHW shifted northward across 49°S quickly enough to lower but not dry the lake, in line with the core evidence presented in Markgraf et al. (2003). There is a corresponding expansion of glaciers at least for the South Patagonian Icefield, from ~6 to 4.4 ka, which were the most extensive of the Holocene, at least at a similar latitude as Cardiel. However, Cardiel appears to remain low slightly later than the Holocene glacier maxima, that is, until ~3.3 ka.

3.3 ka to historic: Virtually all records west of the Andes point to generally colder and wetter conditions (Villagrán and Varela, 1990; Lamy et al., 1999; Jenny et al., 2003) after 3.3 ka, when Lago Cardiel rebounded modestly and fluctuated within 15 m of modern lake levels. This can be interpreted in Figure 8 to reflect passage northward and stabilization of the SHW core at its current position <5° north of the lake (Lawford, 1996). Antarctic SST's continued to cool (Fig. 9c and d) and sea ice expanded (Fig. 9f) sharply with the beginning of the Neo-glacial period (Hodell et al., 2001). At the same time glaciers were generally larger than present in the Andes, but much smaller than their maximum, mid-Holocene extents.

8. Implications for the future

The value of lake shoreline research is that it shows how local hydrologic balance responded to changing regional and global precipitation patterns. In a warming future world, climate models predict a poleward shift and intensification of the SHW (Toggweiler and Russell (2008); IPCC 2013 report). We know that Cardiel can respond quickly to these changes, as evidenced to its rapid expansion 12–11.3 ka as the southern hemisphere rapidly warmed, and the westerlies were likely intense and positioned to the south (Fig. 9e; Anderson et al., 2009). If the past is a guide to the future, we predict that a small temperature increase should dry the lake due to higher evaporation rates and a southward shift the core of the SHW closer to Lago Cardiel. However, in the event of a larger warming of 1–2 °C, the SHW may shift even further south, creating early Holocene-like temperature conditions, and promoting more Atlantic-derived moisture, causing a rise in Lago Cardiel.

There is ample future research opportunity at Lago Cardiel for detailed testing of our lake-level synthesis (Fig. 6) and interpretation (Figs. 7 and 8). Since the pioneering work of Stine and Stine (1990) twenty-six years ago, erosion and flooding have created new exposures along the Rio Cardiel and Rio Bayo, exposing much more of the late Holocene sedimentary record. The near-shore tufa deposits are also extensive, and their rich microstratigraphy is barely tapped by our reconnaissance effort here. These tufas are relatively clean and dense, and would lend themselves well to a concerted dating effort by ^{14}C and ^{238}U-^{230}Th dating. By study of the tufas, it would be especially informative try to fill in the period 30–15 ka, to try to resolve the discrepancies between the shoreline and the core and seismic record (Gilli et al., 2007), and to test in detail the Cardiel record against the record of precipitation changes such as observed by Moy et al. (2008) through the entire Neoglacial period, and Medieval Climate Anomaly and European Little Ice Age intervals of time.

Acknowledgements

We are indebted to the Gary Comer Science and Educational Foundation (CSEF) (Grant Number 8151) for support of this project, and to Wally Broecker and the larger Comer community for all their support and scientific exchange on this and other projects over the years. Adam Hudson provided a very helpful review of an early version. We thank Barbra Quade and Alejandra Borunda for their able assistance in fieldwork, and Audrey Copeland for such diligent processing of the carbon-14 samples. Scott Stine and Adrian Gilli provided very helpful comments that greatly improved the manuscript. We also thank Patricio Moreno for supplying his data from Lago Condorito. Kaplan acknowledges support in part by NSF EAR-0902363. This is LDEO contribution # XXXX.

References

Abbott, M.B., Stafford Jr., T.W., 1996. Radiocarbon geochemistry of modern and ancient lake systems, Baffin Island, Canada. Quat. Res. 45, 300–311.

Agosta, E., Compagnucci, R., Ariztegui, D., 2015. Precipitation linked to Atlantic moisture transport: clues to interpret Patagonian palaeoclimate. Clim. Res. 62, 219–240. https://doi.org/10.3354/cr01272.

Anderson, R.F., Ali, S., Bradtmillller, L.I., Neilson, S.H.H., Fleisher, M.Q., Anderson, B.E.,

Burckle, L.H., 2009. Wind-driven upwelling in the southern ocean and deglacial rise in atmospheric CO_2. Science 323, 1443–1448.
Ariztegui, D., Gilli, A., Anselmatti, F.S., Goni, R.A., Belardi, J.B., Espinosa, S., 2009. Lake-level changes in central Patagonia (Argentina); crossing environmental thresholds for Lateglacial and Holocene occupation. J. Quat. Sci. 25 (7), 1092–1099.
Barros, V.R., Mattio, H.F., 1978. Tendencias y fluctuaciones en la precipitación de la región patagonica. Meteorológica VIII-IX. CAM, Buenos Aires, Argentina, pp. 237–248.
Benson, L.V., Smoot, J.P., Lund, S.P., Mensing, S.A., Foit Jr., F.F., Rye, R.O., 2013. Insights from a synthesis of old and new climate-proxy data from the Pyramid and Winnemucca lake basins for the period 48 to 11.5 cal ka. Quatern. Intern 310, 62–82.
Beres, M., Gilli, A., Ariztegui, D., Anselmati, F.S., 2008. The Lago Cardiel Basin, Argentina (49°S): origin and evolution revealed by high-resolution multi-channel seismi reflection studies. J. S. Am. Earth Sci. 25, 74–85.
Bockheim, J.G., Douglass, D.C., 2006. Origin and significance of calcium carbonate of southwestern Patagonia. Geoderma 136, 751–762.
Brady, A.L., Slater, G.F., Omelon, C.R., Southam, G., Druschel, G., Anderson, D.T., Hawes, I., Laval, B., Lim, D.S.S., 2010. Photosynthetic isotope biosignatures in laminated micro-stromatolitic and non-laminated nodules associated with modern, fresh-water microbialites in Pavillion Lake. B.C. Chem. Geol. 274, 56–67.
Chen, G., Held, I.M., 2007. Phase speed spectra and the recent poleward shift of southern hemispheric surface westerlies. Geophys. Res. Lett. 34 (21), L21805. https://doi.org/10.1029/2007GL031200.
Ciais, P., Petit, J.R., Jouzel, J., Lorius, C., Barkov, N.I., Lipenkov, V., Nicolaiev, V., 1992. Evidence for an early Holocene climatic optimum in the Antarctic deep ice-core record. Clim. Dynam 6, 169–177.
Denton, G.H., Heusser, C.J., Lowell, T.V., Moreno, P.I., Anderson, B.G., Heusser, L.E., Schluchter, C., Marchant, D.R., 1999. Interhemispheric linkage of paleoclimate during the last glaciation. Geogr. Ann. 81 A (2), 107–153.
Divine, D.V., Koc, N., Isaksson, E., Nielsen, S., Crosta, X., Godtliebsen, F., 2010. Holocene Antarctic climate variability from ice and marine sediment cores: insights on ocean-atmosphere interaction. Quat. Sci. Rev. 29, 303–312.
Douglass, D.C., Brockheim, J.G., 2006. Soil-forming rates and processes on quaternary moraines near Lago Buenos Aires. Quat. Res. 65, 293–307.
Fletcher, M.S., Moreno, P.I., 2011. Zonally symmetric changes in the strength and position of the southern westerlies drove atmospheric CO_2 variations over the past 14 k.y. Geology 39 (5), 419–422.
Galloway, R.W., Markgraf, V., Bradbury, J.P., 1988. Dating shorelines of lakes in Patagonia, Argentina. J. S. Am. Earth Sci. 1 (2), 195–198.
Garcia, J.L., Kaplan, M.R., Hall, B.L., Schaefer, J.M., Vega, R., Schwartz, R., Finkel, R., 2012. Glacier expansion in southern Patagonia throughout the Antarctic cold reversal. Geology 40 (9), 859–862.
Garreaud, R.D., 2007. Precipitation and circulation covariability in the extra-tropics. J. Clim. 20, 4789–4797.
Gersonde, R., Crosta, X., Abelmann, A., Armand, L., 2005. Sea-surface temperature and sea ice distribution of the southern Ocean at the EPILOG Last Glacial Maximum—a cicum-Antarctic view based on siliceous microfossil records. Quat. Sci. Rev. 24, 869–896.
Gile, G.H., Peterson, F.F., Grossman, R.B., 1966. Morphological and genetic sequences of carbonate accumulation in desert soils. Soil Sci. 101 (5), 347–360.
Geyh, M.A., Grosjean, M., Nunez, L., Schotterer, U., 1999. Radiocarbon reservoir effect and the timing of the late-glacial/Early Holocene humid phase in the Atacama Desert (Northern Chile). Quat. Res. 52, 143–153.
Gilli, A., Anselmetti, F.S., Ariztegui, D., Bradbury, P., Kelts, K.R., Markgraf, V., McKenzie, J.A., 2001. Tracking abrupt climate change in the southern Hemisphere: a seismic stratigraphic study of Lago Cardiel. Terra nova. 13, 443–448.
Gilli, A., Anselmetti, F.S., Ariztegui, D., Beres, M., McKenzie, J.A., Markgraf, V., 2005a. Seismic stratigraphy, buried beach ridges and contourite drifts: the Late Quaternary history of the closed Lago Cardiel basin, Argentina (49°S). Sedimentol 52, 1–23.
Gilli, A., Ariztegui, D., Anselmetti, F.S., McKenzie, J.A., Markgraf, V., McCulloch, R.D., 2005b. Mid-holocene strengthening of the southern westerlies in South America sedimentological evidences from Lago Cardiel, Argentina (49°S). Glob. Planet. Change 49, 75–93.
Gilli, A., Margraf, V., Anselmatti, F.S., Ariztegui, D., 2007. Comment on: glacier advances east of the southern Andes between the last glacial maximum and 5000 BP compared with lake terraces of the endorrheic Lago Cardiel (49°S, Patagonia, Argentina). Z. Geomorph 49 (4), 433–454.
Govin, A., Michel, E., Labeyrie, L., Waelbroeck, C., DeWilde, F., Jansen, E., 2009. Evidence for northward expansion of Antarctic Bottom Water mass in the Southern Ocean during the last glacial inception. Paleoceanography 24, PA1202. https://doi.org/10.1029/2008PA001603.
Habbeln, D., Marchant, M., Wefer, G., 2002. Paleoproductivity in the southern Peru-Chile current through the last 33,000 years. Mar. Geol. 186, 3–4, 487-504.
Haberle, H., Bennett, K.D., 2004. Post-glacial formation and dynamics of north Patagonian rainforest in the Chonos Archipelago, southern Chile. Quat. Sci. Rev. 23, 2433–2452.
Haberzettl, T., Corbella, H., Fey, M., Jansenn, S., Lücke, A., Mayr, C., Ohlendorf, C., Schäbitz, F., Schleser, G.H., Wille, M., Wulf, S., Zolitska, B., 2007. Lateglacial and Holocene wet-dry cycles in southern Patagonia: chronology, sedimentology, and geochemistry of a lacustrine record from Laguna Potrok Aike, Argentina. Holocene 17 (3), 297–310.
Haberzettl, T., Kuck, B., Wulf, S., Anselmetti, F., Ariztegui, D., Corbella, H., Fey, M., Jansenn, S., Lücke, A., Mayr, C., Ohlendorf, C., Schäbitz, F., Schleser, G.H., Wille, M., Zolitschka, B., 2008. Hydrological variability in southeastern Patagonia and explosive volcanic activity in the southern Andean Cordillera using oxygen isotope stage 3 and the Holocene inferred from lake sediments if Laguna Potrok Aike, Argentina. Palaeogeo. Palaeocl 259, 213–229.
Hall, B.L., Porter, C.T., Denton, G.H., Lowell, T.V., Bromley, G.R.M., 2013. Extensive recession of cordillera Darwin glaciers in southernmost South America during Heinrich stadial 1. Quat. Sci. Rev. 62, 49–55.
Hays, J.D., Imbrie, J., Shackleton, N.J., 1976. Variations in the Earth's orbit: pacemaker of the ice ages. Science 194, 1121–1132.
Hebbeln, D., Marchant, M., Wefer, G., 2002. Paleoproductivity in the southern Peru-Chile Current through the last 33 000 yr. Mar. Geol. 186, 487–504.
Heinsheimer, J.J., 1958. El Lago Cardiel. An. la Acad. Argent. Geogr. 3, 86–132.
Heusser, C., 1989. Polar perspective of late-Quaternary climates in the southern hemisphere. Quat. Res. 32, 60–71.
Heusser, C., 2003. Ice Age Southern Andes: a Chronicle of Paleoecological Events. Elsevier, Amsterdam, Netherlands, 240pp.
Hodell, D.A., Kanfoush, S.L., Shemesh, A., Corsta, X., Charles, C.D., Guilderson, T.P., 2001. Abrupt cooling of Antarctic surface waters and sea-ice expansion in the south Atlantic sector of the southern ocean at 5000 cal Yr B.P. Quat. Res. 56, 191–198.
Hudson, A., Quade, J., Huth, T., Lei, G., Cheng, H., Edwards, R.L., Olsen, J.W., Zhang, H., 2015. Lake-level reconstruction for 12.8-2.3 ka of the Ngangla Ring Tso closed-basin lake system, southwest Tibetan Plateau. Quat. Res. 83, 66–79.
IPCC, 2013. In: Stoker, T.F., Qin, D., Plattner, G.-K., Tignor, M., Allen, S.K., Boschung, J., Naules, A., Xia, Y., Bex, V., Midgley, P.M. (Eds.), Climate Change 2013: the Physical Science Basis. Contribution of Working Group I to the 5th Assessment Report of the Intergovernmental Panel on Climate Change. Cambridge University Press, United Kingdom and New York, NY, USA, 1535pp.
Jenny, B., Wilhelm, D., Valero-Garces, B.L., 2003. The southern westerlies in central Chile; Holocene precipitation estimates based on a water balance model for Laguna Aculeo (33°50'S). Clim. Dynam 20, 269–280.
Kaiser, J., Lamy, F., Hebbeln, D., 2005. A 70-kyr sea surface temperature record off the southern coast of Chile (ODP site 1233). Paleooceanography 20. https://doi.org/10.1029/2005PA001146. PA4009.
Kaplan, M.R., Fogwill, C.J., Sugen, D.E., Hulton, N.R.J., Kubik, P.W., Freeman, S.P.H.T., 2008. Southern Patagonian glacial chronology for the last glacial period and implications for Southern Ocean climate. Quat. Sci. Rev. 27, 284–294.
Kaplan, M.R., Schaefer, J.M., Strelin, J.A., Denton, G.H., Anderson, R.F., Vandergoes, M.J., Finkel, R.C., Schwartz, R., Travis, S.G., Garcia, J.L., Martini, M.A., Nielsen, S.H.H., 2016. Patagonian and southern South Atlantic view of Holocene climate. Quat. Sci. Rev. 141, 112–125.
Kohfeld, K.E., Graham, R.M., de Boer, A.M., Sime, L.C., Wolff, E.W., Le Quéré, C., Bopp, L., 2013. Southern hemisphere westerly wind changes during the last glacial maximum: paleo-data-synthesis. Quat. Sci. Rev. 68, 76–95.
Kutzbach, J., 1980. Estimates of past climate at paleolake Chad, North Africa, based on a hydrological and energy-balanced model. Quat. Res. 14, 210–223.
Lamy, F., Hebbeln, D., Wefer, G., 1999. High-resolution marine record of climatic change in mid-latitude Chile during the last 28,000 years based on terrigenous sediment parameters. Quat. Res. 51, 83–93.
Lamy, F., Kaiser, J., Ninnemann, U., Hebbeln, D., Arz, H.W., Stoner, J., 2004. Antarctic timing of surface water changes off Chile and Patagonian ice sheet changes. Science 304, 1959–1962.
Lamy, F., Kilian, R., Arz, H.W., Francois, J.-P., Kaiser, J., Prange, M., Stenke, T., 2010. Holocene changes in the position and intensity of the southern westerly wind belt. Nat. Geos 3, 695–699.
Lawford, R.G., 1996. North-South variations in west coast hydrometeorological parameters and their significance for Earth Systems. In: Lawford, R.G., et al. (Eds.), High–latitude Rainforests and Associated Ecosystems of the West Coast of America. Springer -Verlag, New York, pp. 3–26.
Markgraf, V., Donson, J.R., Kershaw, P.A., McGone, M., Nichols, N., 1992. Evolution of late Pleistocene and Holocene climates in circum South Pacific land areas. Clim. Dynam 6, 193–211.
Markgraf, V., Bradbury, J.P., Schwalb, A., Burns, S.J., Stern, C., Ariztegui, D., Gilli, A., Anselmatti, F.S., Stine, S., Maidana, N., 2003. Holocene palaeoclimates of southern Patagonia: limnological and environmental history of Lago Cardiel. Holocene 13 (4), 581–591.
Markgraf, V., Whitlock, C., Haberle, S., 2007. Vegetation and fire history during the last 18,000 cal yr B.P. In southern Patagonia: Mallin Pollux, Coyhaique, Province Aisen (45°41'30" S, 71°50'30" W), 640 m elevation. Palaeogeo., Palaeocl 297, 351–366.
Mancini, M.A., Prieto, A.R., Paez, M.M., Schäbitz, F., 2008. Late Quaternary vegetation and climate of Patagonia. Dev. Quat. Sci. 11, 351–367.
Markgraf, V., Uber, U.M., 2010. Late and postglacial vegetation and fire history in southern Patagonia and Tierra del Fuego. Palaeogeo. Palaeocl 297, 351–366.
Masson, V., Vimeux, F., Jouzel, J., Morgan, V., Delmotte, M., Ciaias, P., Hammer, C., Johnsemn, S., Lipenkov, V.Y., Mosley-Thompson, E., Petit, J.-R., Steig, E.J., Stievenard, M., Vaikmae, R., 2000. Holocene climate variability in Antarctica based on 11 ice-core isotopic records. Quat. Res. 54, 348–358.
Mayr, C., Wille, M., Haberzettl, T., Fey, M., Janssen, S., Lücke, A., Ohlendorf, C., Oliva, G., Schübitz, F., Schelser, G.H., Zolitschka, B., 2007. Holocene variability of the southern hemisphere westerlies in Argentinian Patagonia (52°S). Quat. Sci. Rev. 26, 579–584.
McGeehin, J., Burr, G.S., Hodgins, G., Bennett, S.J., Robbins, J.A., Morehead, N.,

Markewich, H., 2004. Stepped-combustion ^{14}C dating of bomb carbon in lake sediment. Radiocarbon 46 (2), 893–900.
Mercer, J.H., 1982. Holocene glacier variation in southern South America. Striae 18, 35–40.
Mohtadi, M., Habbeln, D., 2004. Mechanisms and variations of the paleo-productivity off northern Chile (24°S-33°S) during the last 40,000 years. Paleoceanography 19. https://doi.org/10.1029/2004PA001003. PA2023.
Moreno, P.I., León, A., 2003. Abrupt vegetation changes during the last glacial to Holocene transition in mid-latitude South America. J. Quat. Sci. 18 (8), 787–800.
Moreno, P.I., Videla, J., 2016. Centennial and millennial-scale hydroclimate changes in northwestern Patagonia since 16,000 yr BP. Quat. Sci. Rev. 149, 326–337.
Moreno, P.I., Lowell, T.V., Jacobson, G.L., Denton, G.H., 1999. Abrupt vegetation and climate changes during the last glacial maximum and last termination in the Chilean lake district: a case study from Canal de Puntilla (41°S). Geogr. Ann. 81A (2), 285–311.
Moreno, P.I., Kaplan, M.R., Francois, J.P., Villa-Martínez, R.P., Moy, R.C.M., Stern, C.R., Kubik, P.W., 2009. Renewed glacial activity during the Antarctic cold reversal qand persistence of cold conditions until 11.5 ka in southwestern Patagonia. Geology 37, 375–378.
Moreno, P.I., Francois, J.P., Villa-Martínez, R.P., Moy, C.M., 2010. Co-variability of the Southern westeries and atmospheric CO_2 during the Holocene. Geology 38 (8), 727–730.
Moreno, P.I., Villa-Martínez, R., Cárdenas, M.L., Sagredo, E.A., 2012. Deglacial changes of the southern margin of the southern westerly winds revealed by terrestrial records from SW Patagonia (52°S). Quat. Sci. Rev. 41 (2012), 1–21.
Moreno, P.I., Denton, G.H., Moreno, H., Lowell, T.V., Putnam, A.E., Kaplan, M.R., 2015. Radiocarbon chronology of the last glacial maximum and its termination in northwestern Patagonia. Quat. Sci. Rev. 122, 233–249.
Morrison, R.B., 1965. Quaternary geology of the Great Basin. In: Wright Jr., H.E., Frey, D.G. (Eds.), The Quaternary of the United States. Princeton University Press, Princeton N.J, pp. 265–285.
Moy, C.M., Dunbar, R.B., Moreno, O.I., Francois, J.-P., Villa-Martínez, R., Mucciarone, D.M., Guilderson, T.P., René D. Garreaud, R.D., 2008. Isotopic evidence for hydrologic change related to the westerlies in SW Patagonia, Chile, during the last millennium. Quat. Sci. Rev. 27, 1335–1349.
Oviatt, C.G., Currey, D.R., Sack, D., 1992. Radiocarbon chronology of Lake Bonneville, eastern Great Basin, USA. Palaeogeo. Palaeocl 99, 225–241.
Placzek, C., Quade, J., Patchett, P.J., 2006. Geochronology and stratigraphy of late Pleistocene lake cycles on the southern Bolivian Altiplano: implications for causes of tropical climate change. Geol. Soc. Am. Bull. 118, 515–532.
Placzek, C., Quade, J., Patchett, P.J., 2013. A 130 ka reconstruction of precipitation on the Bolivian Altiplano. Earth Planet. Sc. Lett. 363, 97–108.
Ramos, V.A., 1982. Geología de la Region del Lago Cardiel, Provincia de Santa Cruz. Asoc. Geol. Argent. Rev. XXXVII (1), 23–49.
Rech, J., Pigati, J., Lehman, S.B., McGimpsey, C.N., Grimely, D.A., Nekola, J.C., 2011. Assessing open-system behavior of ^{14}C in terrestrial gastropod shells. Radiocarbon 53 (2), 325–335.
Reimer, P., 2013. IntCal13 and Marine13 radiocarbon age calibration curves 0–50,000 Years cal BP. Radiocarbon 55, 1869–1887.
Rissman, C., Leybourne, M., Benn, C., Christenson, B., 2015. The origin of solutes within the groundwaters of a high Andean aquifer. Chem. Geol. 396, 164–181.
Rumi, A., Gutiérrez, D.E., Núñez, V., Darrigran, G.A., 2008. Malacología latinoamericana. Moluscos agua dulce Argent. Rev. Biol. Trop 56 (1), 77–111.
Schneider, C., Glaser, M., Kilian, R., Santana, A., Butorovic, N., Casassa, G., 2003. Weather observations across the southern Andes at 53°S. Phys. Geogr. 24 (2), 97–119.
Stine, S., Stine, M., 1990. A record from Lake Cardiel of climate change in southern South America. Nature 345, 705–707.
Strelin, J.A., Denton, G.H., Vandergoes, M.J., Ninneman, U.S., Putnam, A.E., 2011. Radiocarbon chronologies of the late glacial Puerto Bandera moraines, southern Patagonian icefield. Argentian. Quat. Sci. Rev. 30, 2551–2569.
Strelin, J.M., Kaplan, M., Vandergoes, M., Denton, G., Schaefer, J., 2014. Holocene glacier chronology of the Lago Argentino Basin, Southern Patagonian icefield. Quat. Sci. Rev. 101, 124–145.
Stuut, J.-B., Lamy, F., 2004. Climate variability at the southern boundaries of the Namib (southwestern Africa) and Atacama (northern Chile) coastal deserts during the last 120,000 yr. Quat. Res. 62, 301–309.
Thompson, D.W.J., Soloman, S., 2002. Interpretation of recent southern hemispheric climate change. Science 296, 895–899.
Timmerman, A., 13 others, 2007. The influence of a weakening of the Atlantic meridional overturning circulation on ENSO. J. Clim. 20, 4899–4919.
Toggweiler, J.R., Russell, J.L., 2008. Ocean circulation in a warming climate. Nature 451, 286–288.
Torfstein, A., Goldstein, S.L., Kagan, E.L., Stein, M., 2013. Integrated multi-site U-Th chronology of the last glacial Lake Lisan. Geochim. Cosmchim. Acta 104, 210–213.
Valero-Garcés, B.L., Jenny, B., Rondanelli, M., Delgado-Huertas, A., Burns, S.J., Veit, H., Moreno, A., 2005. Palaeohydrology of Laguna de Tagua-Tagua (34°30'S) and moisture fluctuations in central Chile for the last 46,000 yr. J. Quat. Sci. 20 (7–8), 625–641.
Villa-Martínez, R., Villagrán, C., Jenny, B., 2003. The last 7500 cal yr B.P. of westerly precipitation in central Chile from a high-resolution pollen record from Laguna Aculeo (34°S). Quat. Res. 60, 284–293.
Villa-Martínez, R., Moreno, P.I., Valenzuela, M., 2012. Deglacial and post-glacial vegetation changes on the eastern slopes of the central Patagonian Andes (47°S). Quat. Sci. Rev. 32, 86–99.
Villagrán, C., 1990. Glacial climates and their effects on the history of the vegetation of Chile: a synthesis based on palynological evidence from Isla de Chiloe. Rev. Palaeob. Palynol. 65, 17–24.
Villagrán, C., Varela, 1990. Palynological evidence for increased aridity on the central Chilean Coast during the Holocene. Quat. Res. 34, 198–207.
Wenzens, G., 2005. Glacier advances east of the southern Andes between the last glacial maximum and 5000 BP compared with lake terraces of the endorrheic Lago Cardiel (49°S, Patagonia, Argentina). Z. Geomorph 49 (4), 433–454.
Wenzens, G., 2006. Terminal moraines, outwash plains, and lake terraces in the vicinity of Lago Cardiel (49°S: Patagonia, Argentina)—evidence for Miocene Andean foreland glaciations. Arct. Antarct. Alp. Res. 38 (2), 276–291.
Wille, M., Maidana, N.I., Schäbitz, F., Fey, M., Haberzetl, T., Jansenn, S., Lücke, A., Mayr, C., Ohlendorf, C., Schleser, G.H., Zolitschka, B., 2007. Vegetation and climate dynamics in southern South America: the microfossil record of Laguna Potrok Aike, Santa Cruz, Argentina. Rev. Palaeob. Palynol. 146, 234–246.